

CROSSING THE PHASE TRANSITION IN STRONG-FOCUSING PROTON SYNCHROTRONS

A. SØRENSEN†

MPS Division, CERN, Geneva, Switzerland

(Received February 11, 1974; in final form April 8, 1974)

Two effects are observed when a high-intensity bunch crosses the phase transition: bunch-length oscillations are excited, and there is also a sudden increase of the longitudinal emittance. These effects may for some accelerators be an intensity limitation as important as the transverse space-charge limit at injection. The bunch-length oscillations are caused by longitudinal space-charge forces and their nature is well understood. The emittance increase is less well understood, the most important mechanism is probably a negative-mass instability which develops right after transition, but also other mechanisms play a certain role. Various cures exist to counteract these mechanisms; the most successful one is the so-called $\gamma_{\text{transition}}$ -jump, where the transition energy is rapidly reduced by pulsing a suitable set of quadrupoles. The various mechanisms and cures are first discussed in qualitative terms, then the theory is developed, and at the end the state of today's knowledge is discussed.

CONTENTS

	<i>Page</i>
1 THE PURPOSE OF THIS PAPER	142
2 OBSERVED PHENOMENA AND QUALITATIVE EXPLANATIONS	143
2.1 Experiments	143
2.2 Why there is a Phase Transition	143
2.3 Can Transition Energy be Removed?	144
2.4 The Radio Frequency System	145
2.5 Longitudinal Space-Charge Forces	145
2.6 Mechanisms for Longitudinal Emittance Blow-Up	146
3 QUALITATIVE DESCRIPTION OF CURES	147
3.1 Why the Effects may be Harmful	147
3.2 Artificial Blow-Up Before Transition	147
3.3 Triple Switch	147
3.4 Continuous Rf Matching	147
3.5 Wall Modifications	147
3.6 Feedback	148
3.7 $\gamma_{\text{transition}}$ -jump	148
4 EQUATIONS OF MOTION FOR A SINGLE PARTICLE	149
4.1 What to Include	149
4.2 Basic Equations	149
4.3 Longitudinal Space-Charge Forces	150
4.4 Transverse Space-Charge Forces	151
4.5 $\gamma_{\text{transition}}$ -jump	153
4.6 Nesting it All Together	153
5 EQUATION OF MOTION FOR THE BUNCH (VLASOV EQUATION)	154

† Present address: Regnesentret, Universitetet i Trondheim, Trondheim, Norway.

6 ELLIPSE DESCRIPTION OF THE BUNCH MOTION	155
6.1 What such a Simple Description Can Give Us	155
6.2 Linearization of the Single-Particle Equations	155
6.3 Equations of Motion for an Elliptic Bunch	157
6.4 Interpretation of the Bunch Variables	158
6.5 Connection between the two Space-Charge Parameters N_0 and $\eta_0(0)$	158
6.6 Hamiltonian Formulation of the Bunch Equations	160
6.7 Numerical Calculations	160
7 SUPER-PARTICLE DESCRIPTION OF THE BUNCH MOTION	161
7.1 The Super-Particle Method	161
7.2 Longitudinal Space-Charge Forces and the Negative-Mass Instability	161
7.3 Transverse Space-Charge Forces	162
8 EXPANSION-TYPE DESCRIPTION OF THE BUNCH MOTION	163
8.1 The Expansion Method	163
8.2 Numerical Calculations on the Negative-Mass Instability	165
9 SOME OTHER MECHANISMS AND ONE MORE CURE	166
9.1 Recapitulation	166
9.2 The Influence of Sextupolar Magnetic Fields	166
9.3 Coupling between Betatron Oscillations and Synchrotron Oscillations	168
9.4 Coupling to the Rf Cavities ("Beam Loading")	169
9.5 Continuous Rf Matching	170
10 THE STATE OF TODAY'S KNOWLEDGE	171
ACKNOWLEDGEMENTS	172
REFERENCES	172

1 THE PURPOSE OF THIS PAPER

Shortly after the strong-focusing principle had been invented, it was discovered that the longitudinal stability is of one type at injection energy and of the opposite type at top energy. In the first part of the acceleration cycle the particles have to ride in front of the crest of the rf wave, as behind the crest they would be unstable. In the last part of the cycle the particles have to ride behind the crest of the wave, as now they would be unstable if in front of the crest. Somewhere between injection energy and top energy the nature of the stability changes. This point is called the phase transition. The reason for the name is that the phase of the rf wave has to be shifted to retain stability of the particles. For brevity one often just says transition.

The particle dynamics at transition in the absence of space-charge forces has been known¹⁻³ since 1953. However, for some reason, more than 10 years passed with no attempt to include space-charge forces in the dynamics, even though these forces may be quite strong at phase transition and modify the dynamics considerably.

In the last few years a substantial amount of

work has been done on the crossing of the phase transition with an intense beam. This includes not only theoretical studies on the beam dynamics, but also more refined experimental work than was previously available, proposals of methods to compensate various harmful effects, and the detailed engineering and testing of such proposed methods.

However, much of this information is difficult to get hold of, as it is scattered around in internal reports in various laboratories. It adds to the difficulties that they use different terminologies, different notations and different languages.

The purpose of this paper is to make the present knowledge on the transition problem available to people building, operating or trying to improve accelerators.

Section 2 describes the mechanisms that cause the observed effects, and Section 3 describes some proposed cures for them; both these sections are elementary and use no mathematics. The theory is developed in Sections 4 to 9. Section 10 tries to assess the present knowledge. Experimental results, if available, are given along with the theoretical results.

2 OBSERVED PHENOMENA AND QUALITATIVE EXPLANATIONS

2.1 Experiments

When an intense beam crosses transition, two effects are observed⁴:

- i) Bunch-length oscillations are excited.
- ii) The longitudinal emittance is rapidly increased.

Both phenomena disappear gradually when the intensity is reduced.

Figure 1 shows the signal from a broad-band pick-up electrode in the CERN PS. The injection into the machine was done in such a way that not all bunches contained the same number of particles.

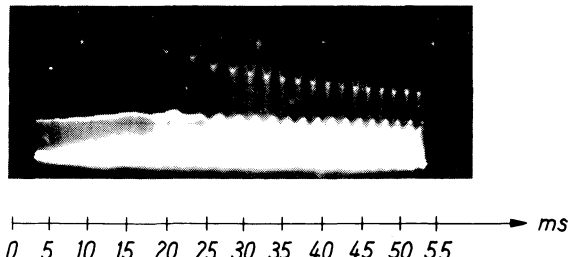


FIGURE 1 One high-intensity and one low-intensity bunch, picked out by an electronic gate. Bandwidth 80 MHz.

By means of an electronic gate only the signals from one high-intensity and one low-intensity bunch are displayed on the oscilloscope, while the signals from all other bunches are blocked out. The low-intensity bunch shows neither bunch-length oscillations nor emittance blow-up; the high-intensity bunch shows both. Having both signals on the same picture excludes that the whole thing is only an instrumental effect, like the saturation of an amplifier, for instance.

In Figure 2 the signal from only one bunch has been permitted through the gate, and this only once every 150 revolutions. This gated signal is then shown in a mountain-range display. The sweep is triggered from the rf signal; the shift of the rf phase at transition therefore appears as if the bunch is shifted in position. In addition to what we saw in Figure 1, we can now also see that the bunch sometimes has strange shapes after transition, for example two maxima. Figure 2 has been composed of several photos, taken at different machine cycles.

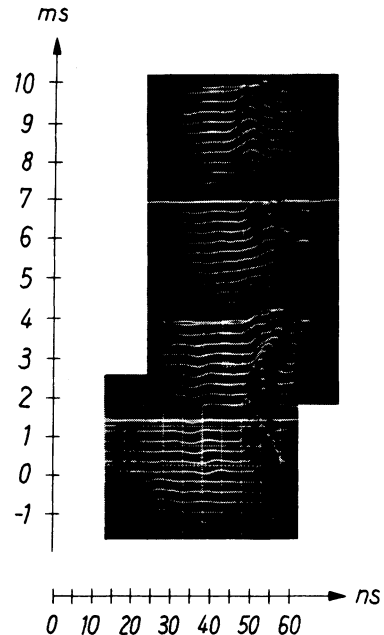


FIGURE 2 One high-intensity bunch shown once every 150 turns in mountain-range display. Bandwidth 150 MHz.

2.2 Why there is a Phase Transition

Let us imagine two particles travelling around in a synchrotron, one of them having slightly more energy than the other one. Which one has the larger angular velocity? Of course the most energetic one has the larger ordinary velocity, but that is at least partly compensated by the somewhat greater orbit radius, caused by the greater centrifugal force, see Figure 3. It is not evident which of the two effects will dominate. Denoting the velocity by v and the radius by R , the angular velocity is $\omega = v/R$. The answer to our question depends on

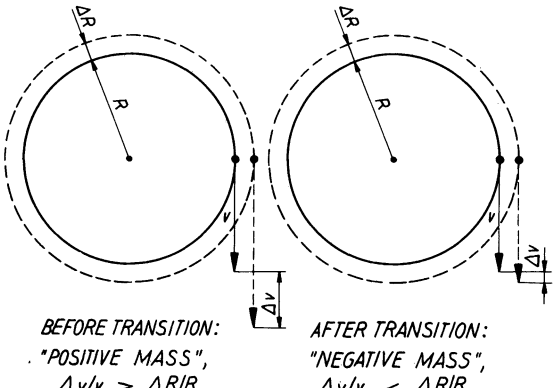


FIGURE 3 "Positive mass" and "negative mass."

whether $\Delta v/v$ is greater or smaller than $\Delta R/R$. If $\Delta v/v$ is the greater quantity, the velocity difference will dominate, and the energetic particle gets faster around the machine. If $\Delta R/R$ is the greater quantity, the energetic particle will need more time than the other to get around the machine.

This latter situation seems somewhat paradoxical: push a particle forwards, and it will move backwards relative to its undisturbed neighbours; push it backwards, and it will move forwards. It is as if the particles had negative mass. However, this negative-mass situation is not at all unique to strong-focusing proton synchrotrons. Electron synchrotrons operate in this regime all through the acceleration cycle, and so do weak-focusing proton synchrotrons. But the situation is also known outside the field of accelerators. A satellite that loses energy by entering into the earth's atmosphere, will have a shorter period than before, not longer. A similar situation governs the particles that make up Saturn's rings: as gravity is an attractive force, the particles will effectively repel each other due to the "negative mass," therefore the rings are very evenly populated. (This was first found by Maxwell⁵ in 1856.) In accelerators things are not always so favourable: equally charged particles repel each other, in the negative-mass regime they will effectively attract each other. Under certain circumstances the situation gets unstable, and all the particles tend to lump together at the same place. This is often called the negative-mass instability.

For a given energy difference between the two particles under comparison, the $\Delta v/v$ depends only on their energy and is completely defined by relativistic dynamics alone: for large energies ($E \gg mc^2$) the $\Delta v/v$ becomes very small. The $\Delta R/R$ depends also upon the focusing properties of the machine: the stronger focusing, the smaller $\Delta R/R$.

As a result, for a machine with a given focusing, the situation is as follows: at the beginning of the acceleration, the "mass" is positive, at top energy, the "mass" is negative. The stronger the focusing, the higher is the energy at which the velocity change will lose the competition with the radius change. In other words: the stronger the focusing, the higher is the transition energy. For a strictly circular machine, $\gamma_{\text{transition}} = Q_H$, where γ denotes the relativistic mass ratio E/mc^2 and Q_H denotes the number of horizontal betatron oscillations per turn. If the orbits deviate substantially from a circle, $\gamma_{\text{transition}}$ may deviate appreciably from Q_H .

Right at transition a particle will not (to the

first order) be azimuthally displaced relative to the other ones whether you push it forwards or backwards, or not at all. It is as if the mass were infinite.

Because the apparent mass gets very large when transition is approached, the amplitude of the longitudinal oscillations will become very small. Therefore the bunches are very short at transition.

2.3 Can Transition Energy be Removed?

It is possible to choose the parameters of a strong-focusing synchrotron in such a way that there will be no phase transition inside its range of operation; thus the CERN PS Booster is actually built this way: injection is at 50 MeV and ejection is at 800 MeV, while transition is way up at 4.5 GeV. For larger machines this usually leads to a somewhat awkward set of parameters.

The Serpukhov machine was originally planned so that it would always have the below-transition type of stability. The transition energy would be pushed very high up, or one could even make it imaginary. The method was to introduce reverse bending⁶ in some places around the circumference. The price one would have to pay for this was a substantial reduction in the machine's top energy. The idea was finally dropped, and as a result the top energy of the machine is now about 75 GeV, rather than about 50 GeV as it would have been with the other scheme.

A variant of the reverse-bending scheme is to introduce long straight sections⁷ with a phase advance close to π . In machines where a large fraction of the circumference is free from magnets, as is often the case with boosters, this may be a practical method. Some long straight sections are useful anyway. The method leads, however, to quite large excursions of the momentum compaction function.

It can be shown³ that if the magnet lattice is composed of sectors in all of which the radius of curvature is the same, separated by empty straight sections, $\gamma_{\text{transition}} \approx Q_H$. Therefore, all schemes in which $\gamma_{\text{transition}}$ is pushed very high up must rely upon a substantial deviation from circular orbits.

For the CERN SPS the possibility of operating entirely above transition, as one does with electron synchrotrons, was seriously considered. This would, however, lead to uncomfortably low Q -values, meaning a wide vacuum chamber, and its injector (the PS) would have to work at uncomfortably high energies, meaning a low cycling rate. These

disadvantages would outweigh the advantage of getting rid of the transition.

At NAL the transition is also crossed, in the Booster as well as in the Main Ring.

One can get rid of the transition, but it is usually not worth the price.

2.4 The Radio-Frequency System

Before transition, when the "mass" is positive, the particles have to ride in front of the crest of the rf wave which one can imagine is travelling around the machine. See Figure 4. If a certain particle has

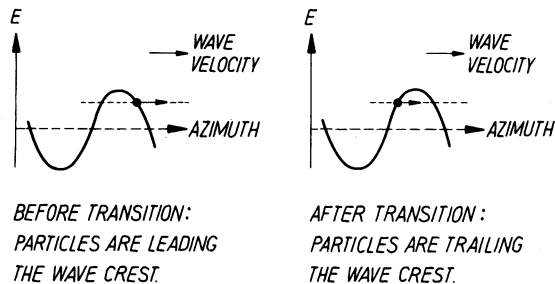


FIGURE 4 Phase stability before and after transition. E denotes the longitudinal electric field, shown as a function of azimuth at a given time.

come in front of the other ones, it will see a smaller field and will therefore slow down with respect to the others. If the particle has come somewhat behind the other ones, it will see a stronger field which finally will make it catch up with the others. The particles can therefore execute stable oscillations around the so-called phase-stable point (provided that the deviations from the correct position and momentum are not so large that the particle drops off the wave). At the corresponding point behind the crest, the particles would evidently be unstable, by the same sort of argument.

After transition, when the "mass" is negative, the particles have to ride behind the crest of the wave, see again Figure 4. If now a particle has come in front of the others, it will see a larger field, but due to the "negative mass" it will then be accelerated less than the other ones. If behind the others, it will see a smaller field, giving more acceleration.

At transition, where the stability changes from one type to the other, the phase of the rf wave must be rapidly shifted relative to the bunch of particles. This is normally done by running the rf cavities at a "wrong" frequency for a very short

time. The timing of this so-called rf switch must in most machines be accurate to about a millisecond. The reason why this is not more critical is that, due to the apparently infinite mass, the phase oscillations are completely frozen at transition, and they are very slow in the neighbourhood of transition.

Other methods of crossing transition have also been proposed. One such method, called "ducking under," consists in reducing gently the amplitude of the rf wave while simultaneously sliding its phase in such a way that the particles get the right amount of acceleration all the time. When the particles are sitting right at the top of the wave, one gradually starts to increase the rf amplitude, still letting the wave slide in the same direction as before. This method, and various proposed modifications to it, do not appear to have any advantages over the simple phase switch. Their properties are less well known.

2.5 Longitudinal Space-Charge Forces

In the previous paragraph we saw that in order that the particles remain stable after transition, we somehow have to change the longitudinal focusing properties of the rf system. How will the situation be modified by longitudinal space-charge forces⁸?

Particles of the same charge always repel each other. Therefore, they counteract the rf forces before transition and help the rf forces above transition. The result of this is that below transition the equilibrium bunch length is larger with space-charge forces than without, and above transition the equilibrium bunch length is shorter with space-charge forces than without. Close to transition the concept of an equilibrium bunch length is not very meaningful. Figure 5 shows the equilibrium bunch length with and without space-charge forces as a function of time. The origin of time is chosen at transition.

Imagine a bunch which starts in an equilibrium (nonoscillating) condition far before transition. Outside a region around transition the conditions

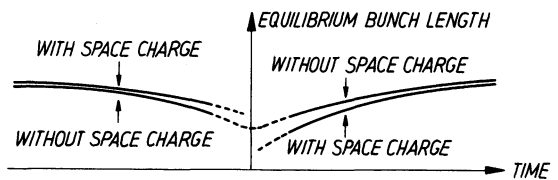


FIGURE 5 Equilibrium bunch length with and without longitudinal space-charge forces.

in the machine change slowly compared to a period of the synchrotron oscillations and the bunch is able to adjust itself to the changing conditions, and the bunch will stay in equilibrium. At transition the synchrotron frequency goes to zero and all motion is "frozen." Just above transition, therefore, the bunch is still longer than the equilibrium length would have been if there were no space-charge forces, see Figure 6, while the true equilibrium length is shorter than this. The bunch will therefore make itself shorter to approach equilibrium, overshoot, and start oscillations around its equilibrium length. Figure 6 shows the bunch length as a function of time, assuming linear space-charge forces.

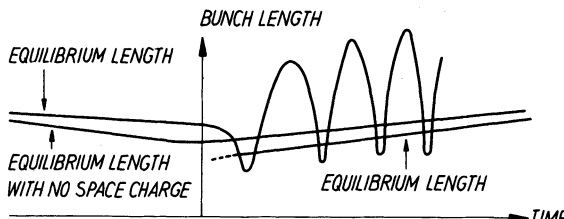


FIGURE 6 Bunch length as a function of time, assuming linear space-charge forces.

2.6 Mechanisms for Longitudinal Emittance Blow-Up

The arguments given in the previous paragraph explain why bunch-length oscillations are excited when crossing transition, but it does not at all explain why there is an emittance blow-up at transition. A detailed calculation⁸ including linear longitudinal space-charge forces (Section 6) predicts quantitatively all the essential features of the oscillations: amplitude, phase, the rapidity with which the oscillations start,⁸ and their response to manipulation with machine parameters.⁹ But such a theory also predicts that the longitudinal emittance is strictly conserved.

In reality, the blow-up is quite large: for instance, Figure 1 of Ref. 10 shows that with 1.4×10^{12} protons in the CERN PS, the average bunch length increases with about a factor 1.5. This corresponds to an increase of longitudinal emittance with about a factor 2. The whole blow-up process lasts only a millisecond or two. For a long time it remained a mystery how any sort of nonlinearity could cause such a *rapid* blow-up, though it was well known that nonlinearities can increase the

emittance by filamentation, which is a slow process.

It now appears that the increase of emittance is caused by a mixture of several effects.

The most important one is probably a negative-mass instability which appears right after transition.^{11,12} During a short period of time, right after the transition is crossed, the energy spread of the bunches is not sufficiently large to keep the bunches stable. A negative-mass instability will develop until stability is again reached. The beam becomes stable due to two reasons: the instability kills itself by increasing the energy spread, thus enhancing the Landau damping; moreover, the bunches get more stable as they get further away from transition.

Another effect^{13–15} that may play a role in some accelerators is the spread of $\gamma_{\text{transition}}$ by transverse space-charge forces ("Umstätter effect"). Particles in the middle of the bunch suffer a large Q -depression due to the transverse space-charge forces, and along with the Q -depression goes a similar depression of $\gamma_{\text{transition}}$. The corresponding depressions are negligible for particles at the two ends of the bunch. Therefore, some particles will cross transition earlier than they otherwise would do, while other particles are only little affected in this way. No single timing of the phase jump can therefore make all particles happy, and emittance blow-up is the result.

Coupling between the beam and the rf cavities¹⁶ may have an effect similar to the coupling between the beam and the vacuum chamber, but with less short-wavelength structure.

For machines with a large energy spread at transition, and therefore a large contribution from synchrotron oscillations to the horizontal beam size, the coupling to sextupolar magnetic fields^{14,17–19} may also cause blow-up. Low-energy particles and high-energy particles cannot agree on when the transition is actually crossed.

The nonlinearity of the imposed rf field can also cause blow-up.

Coupling between synchrotron oscillations and betatron oscillations²⁰ will normally average out so as to give no important contribution to the longitudinal dynamics. In a region around transition, where the synchrotron oscillations are very slow, this averaging process does not work as normally, and the coupling term will integrate to a nonzero contribution. Particles with large betatron amplitudes will go through transition in a way slightly different from particles with small betatron amplitudes.

3 QUALITATIVE DESCRIPTION OF CURES

3.1 Why the Effects may be Harmful

In Section 2 we have discussed two effects that appear when crossing transition, namely bunch-length oscillations and emittance blow-up. Depending on circumstances, these effects may be harmful in various ways, for example:

- i) Particles may be lost out of the rf bucket.
- ii) Longer bunches means shorter space between them, therefore fast kickers must be even faster.
- iii) Because of the increased contribution from energy spread to the horizontal beam dimension, particles may be lost against the vacuum chamber.
- iv) For the same reason, the beam jump at a septum for slow or fast ejection must be larger.
- v) If the accelerator is to feed a pair of storage rings, the interaction rate in these rings is (under certain conditions) proportional to the square of the phase-space density in the longitudinal phase space.

In the next paragraphs we shall describe some cures that have been suggested. Some of them work, some of them do not, some of them have not been sufficiently investigated to say whether they will work or not. We describe also the unsuccessful cures to avoid unnecessary re-invention.

3.2 Artificial Blow-Up Before Transition

The space-charge parameter is proportional to the longitudinal emittance to the power $-3/2$. If the space-charge parameter is very large, it may pay²¹ to blow up the bunches artificially by beam gymnastics and subsequent filamentation before transition, in the sense that the artificial-plus-transition blow-up is less than the transition blow-up alone with a very large space-charge parameter. This rather crude method should not be used if phase-space density is at a premium.

No experiments have been done.

3.3 Triple Switch

This is a method^{8,22,23} intended to compensate for the bunch-length oscillations only, not for the blow-up. The rf phase is switched three times instead of only once. We jump to the unstable

phase for a short while in order to create an oscillation with such a phase and amplitude that it will exactly cancel the oscillations set up by the space-charge forces. The location of the unstable interval gives the phase and its duration gives the amplitudes of the oscillations created.

The method has been tried on the CERN PS without much success.^{24,25} The reason for this seems to be that the rf defocusing introduced keeps the bunches long, but with low energy spread. This reduces the Landau damping. The negative-mass instability is therefore aggravated.¹¹ On oscilloscopes the bunch envelope looks more blurred than without triple switch.²⁵

3.4 Continuous Rf Matching

Up to transition the normal rf programme is used. After transition the amplitude and phase of the rf system are adjusted so as to keep the acceleration ($V \sin \phi_s$) constant and let the focusing ($V \cos \phi_s$) change in such a way that for every instant of time the sum of the rf focusing force and the space-charge force is the same as it was at the corresponding instant before transition.

This method is very sensitive to intensity fluctuations and to small errors in the rf programme.²⁶ No experiments have been done.

3.5 Wall Modifications

Reactive loading of the vacuum-chamber walls may reduce both effects by reducing (ideally to zero) the space-charge forces themselves. Such loading may be achieved by a thin dielectric layer inside the vacuum chamber,²⁷ by shallow corrugations of the walls,^{27,28} or by helical inserts.²⁹ The space-charge forces are proportional to the difference between electrically and magnetically stored energy in the beam/vacuum chamber system; that is, proportional to

$$g = 1/C - \beta^2 L \quad (3.1)$$

where C is the capacitance per unit length and L the inductance per unit length. For walls of uniform cross section $1/C = L$ and $g > 0$ at all energies. Wall modifications, such as those mentioned, can increase C or L so as to make $g = 0$ at transition. This would at one blow eliminate both these effects.

It is particularly welcome that this method would be independent of bunch-to-bunch fluctuations and pulse-to-pulse fluctuations.

It is important not to overcompensate, as overcompensation is worse than undercompensation.⁸ If $\beta \approx 1$, as is normally the case at transition, only a small modification of C or L is necessary. Thus a dielectric lining will typically be 1 cm thick, or corrugations of the wall typically 1 cm deep if applied along the whole circumference of the machine. A helical insert will typically occupy a few metres of straight section.

In the negative-mass instability,³⁰ the fastest-growing mode has a wavelength which is of the order of $\lambda \sim d/\gamma$, where d is a characteristic transverse dimension of the vacuum chamber and γ is the relativistic mass factor. At transition λ is typically 1 cm. The frequency response of such wall modifications at very high frequencies is therefore important. This problem has not been sufficiently analysed; especially for lumped structures it must be a serious problem.

No experiments have been made.

3.6 Feedback

The bunch-length oscillations are detected by a pick-up electrode, and this information is fed back into the rf system. In this way the bunch-length oscillations are damped down to a negligible amplitude. However, this method cannot prevent large bunch-length oscillation from appearing right after transition; the feedback can only damp the oscillations after they have been excited. During the time that the feedback needs to stop the oscillations, filamentation may dilute the phase space, or particle loss out of the bucket or against the vacuum chamber may occur.³¹

Feedback has been tried successfully on the Brookhaven AGS³² and on the CERN PS,³³ but in both cases the oscillations to be damped were caused by other things than the crossing of phase transition.

3.7 $\gamma_{\text{transition}}\text{-jump}$

Crossing transition fast is better than crossing it slowly. The reason is that fast crossing does not give the bunches time enough to get very short, and therefore the space-charge forces get smaller than with slow crossing and very short bunches. However, in most accelerators it is not possible to boost the rate of acceleration in a range around transition.

The $\gamma_{\text{transition}}\text{-jump}$ is an alternative way of achieving a fast crossing of transition.³⁴ One manipulates the focusing properties of the machine

so as to make $\gamma_{\text{transition}}$ time-dependent. A set of quadrupole magnets is pulsed at transition in such a way that $\gamma_{\text{transition}}$ is rapidly reduced, as shown in Figure 7.

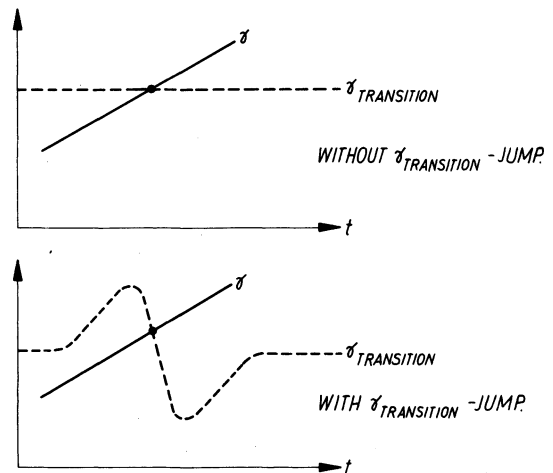


FIGURE 7 Speeding up the crossing of transition by a $\gamma_{\text{transition}}\text{-jump}$.

If the pulsed quadrupoles are located at proper places in the magnet lattice, it is possible to change $\gamma_{\text{transition}}$ without changing the Q -values.³⁵ Some of the pulsed quadrupoles must then be focusing while others are defocusing. An early version of the $\gamma_{\text{transition}}\text{-jump}$ method, using only one type of quadrupoles, was called the Q -jump method, as the horizontal Q -value was changed together with $\gamma_{\text{transition}}$. This is normally not desirable, and at least the Q -values must not be pushed into a stop-band.

The $\gamma_{\text{transition}}\text{-jump}$ method decreases the longitudinal space-charge forces themselves (though not to zero), and it therefore helps against emittance blow-up as well as against bunch-length oscillations. It also reduces the effect of the coupling to cavities. As the bunches are not so short, the transverse space-charge forces are also reduced, and thereby the spread of $\gamma_{\text{transition}}$ due to transverse space-charge forces. As the bunches have less momentum spread, the $\gamma_{\text{transition}}\text{-jump}$ will also help against the effect of sextupolar magnetic fields.

Variations of the theme,^{9,36-40} introducing various sorts of asymmetric jumps, can in the same go achieve better bunch-length matching and thereby reduce bunch-length oscillations even further than indicated by the reduction of the space-charge forces alone.

The method has been successfully tried on the CERN PS¹⁰ and is now used in daily operation.

4 EQUATIONS OF MOTION FOR A SINGLE PARTICLE

4.1 What to Include

In Section 2 are discussed various mechanisms that contribute to the observed bunch-length oscillations and emittance blow-up, and in Section 3 are discussed various cures proposed to combat these undesirable effects. The mechanisms discussed are:

- 1) longitudinal space-charge forces (a: linear, and b: nonlinear),
- 2) transverse space-charge forces (=“Umst tter effect”),
- 3) rf nonlinearities,
- 4) influence of sextupolar magnetic fields,
- 5) coupling to the rf cavities (=beam loading),
- 6) coupling between betatron oscillations and synchrotron oscillations.

The cures discussed are:

- 7) $\gamma_{\text{transition}}$ -jump,
- 8) triple switch (or rather: multiple switch),
- 9) continuous rf matching,
- 10) wall modifications,
- 11) feedback,
- 12) artificial blow-up.

The most systematic approach would be to develop a theory which takes into account all mechanisms and all cures in one go, but this would be a rather heavy mathematical machinery. On the other hand it would not be satisfactory to treat each mechanism by itself and each cure by itself; a cure must be evaluated along with the mechanism which it is supposed to compensate. Now, some cures are like broad-banded antibiotics; they help against many diseases at once: the $\gamma_{\text{transition}}$ -jump helps against bunch-length oscillations and against the negative-mass instability (both of which are caused by longitudinal space-charge forces), and it also helps to reduce the spread of $\gamma_{\text{transition}}$ due to transverse space-charge forces. The triple switch helps against the bunch-length oscillations, but it aggravates the

negative-mass instability. Perhaps there is an optimum somewhere?

In this section we derive equations of motion that take into account longitudinal and transverse space-charge forces and rf nonlinearities in a machine with $\gamma_{\text{transition}}$ -jump and multiple phase switch. In Sections 5–8 these equations of motion are handled to various degrees of accuracy. Towards the end, in Section 9, we shall return to some of the other points of the list above.

This is an arbitrary compromise. It could, for instance, be interesting to look at beam/cavity interaction in connection with $\gamma_{\text{transition}}$ -jump and multiple phase switch, as this interaction is important in some accelerators and its effect may be reduced by both cures. However, the best mathematical model for such an interaction will depend on how the cavity is built. The important point is how the coupling impedance varies with frequency. Cavities usually have higher resonances, and the positions and strengths of these resonances depend on how the cavity is constructed. It is therefore difficult to include beam/cavity interaction in a way which is generally valid for any machine. Another mechanism which might be interesting to include is the coupling to sextupolar magnetic fields, as this coupling is also influenced by a $\gamma_{\text{transition}}$ -jump as well as by multiple phase switch. However, the influence of sextupolar magnetic fields is important in machines with large longitudinal emittance, while the space-charge effects are important in machines with small longitudinal emittance. They are rarely important at the same time. We therefore include points (1), (2), (3), (7) and (8) in a coherent theory, and rather come back to some of the other problems.

4.2 Basic Equations

Our starting point will be Eqs. (5.5a) and (5.5b) of Courant and Snyder:³

$$\frac{d}{dt} \left(\frac{\Delta E}{\omega_s} \right) = \frac{eV}{2\pi} (\sin \phi - \sin \phi_s), \quad (4.1)$$

$$\frac{d\phi}{dt} - \omega_1 = \frac{\eta h \omega_s}{\beta^2} \frac{\Delta E}{E}. \quad (4.2)$$

Here ΔE denotes the energy difference between the particle in question and the synchronous particle, ω_s is the angular velocity of the particle, eV is the energy gain per turn at the crest of the rf wave, h is the harmonic number (i.e. the applied frequency is designed to be h times the particle

frequency), and ω_1 is the frequency error (i.e. the difference between the actual applied frequency and its ideal value $h\omega_s$). In the following we shall assume $\omega_1 = 0$. The quantity denoted by

$$\eta = \frac{p}{T} \frac{dT}{dp}, \quad (4.3)$$

where p is the momentum of the particle and T is its revolution time, obeys the equation [see Eq. (5.3) of Ref. 3]:

$$\eta = \left(\frac{mc^2}{E_{\text{transition}}} \right)^2 - \left(\frac{mc^2}{E} \right)^2, \quad (4.4)$$

where E is the energy of the particle and $E_{\text{transition}}$ is a constant of the machine called the transition energy. We notice that $\eta < 0$ before transition, $\eta = 0$ at transition and $\eta > 0$ after transition. $1/\eta$ is a measure of the “stiffness” of the particle against longitudinal forces. ϕ is the phase of the particle in question and ϕ_s is the phase of the synchronous particle. The difference $\phi - \phi_s$ we shall in the following frequently denote by θ . The sign convention used for ϕ (and for ϕ_s) is as follows: one imagines an rf wave travelling around the machine, and ϕ is then taken to be the phase in rf radians by which the particle is *lagging behind* this wave, measured from a cross-over.

The solution of Eqs. (4.1), (4.2) is well known,^{1–3} but we shall now modify these equations of motion to include the driving mechanisms (1), (2), (3) and the cures (7), (8) of Subsection 4.1.

4.3 Longitudinal Space-Charge Forces^{8,21,41}

Let $E_\theta(\theta)$ denote the longitudinal (index θ) electric field caused by space charge, measured at the point θ (argument θ). As always with transition problems we shall have to be careful about sign conventions: $E_\theta(\theta)$ is taken to be positive when accelerating, negative when decelerating. The energy gain per turn is then

$$eV \sin \phi + eE_\theta(\theta)2\pi R_{\text{mach}}$$

instead of $eV \sin \phi$ as it was in the absence of space charge. Equation (4.1) must therefore be replaced by

$$\frac{d}{dt} \left(\frac{\Delta E}{\omega_s} \right) = \frac{eV}{2\pi} (\sin \phi - \sin \phi_s) + eE_\theta(\theta)R_{\text{mach}}. \quad (4.5)$$

R_{mach} is the radius of the machine.

The longitudinal field $E_\theta(\theta)$ will evidently depend on how the electric charge is distributed along the bunch. With $\lambda(\theta)$ denoting the number of particles per rf radian at θ , we shall now establish the relationship between $\lambda(\theta)$ and $E_\theta(\theta)$.

The potential $U(\theta)$ is found by performing an integral

$$U(\theta) = \int_{-\infty}^{\infty} K(\theta' - \theta)\lambda(\theta') d\theta'. \quad (4.6)$$

For a cylindrical bunch inside a cylindrical pipe with infinite conductivity the kernel is according to Morton⁴² to a very good approximation equal to

$$K(\theta' - \theta) = D \exp(-\Lambda|\theta' - \theta|). \quad (4.7)$$

The characteristic strength of the kernel is D and its characteristic width in rf radians is $1/\Lambda$. Measured in distance along the circumference, the characteristic width³⁰ is of the order d/γ , where d is a typical transverse dimension of the pipe and γ is the relativistic mass ratio E/mc^2 . For the CERN PS, d is about 7 cm and γ is about 6 at transition, therefore d/γ is about 1 cm in this machine, while the bunches are about 3 m long. For most machines the kernel width is small compared to the bunch length. If one is not interested in features shorter than the kernel width, one may replace the kernel (4.7) with a delta function of suitable strength.

The distance along the circumference of the machine is

$$s = \frac{R_{\text{mach}}}{h} \theta. \quad (4.8)$$

The density of particles per unit of azimuthal length is therefore

$$\frac{h}{R_{\text{mach}}} \lambda(\theta). \quad (4.9)$$

We define a quantity g_0 by requiring the capacity between beam and vacuum chamber to be

$$C = \frac{4\pi\epsilon_0}{g_0} \quad (4.10)$$

per unit length. For most practical purposes one may take⁴¹ $g_0 \approx 4.5$ slightly dependent on the transverse dimensions and on the assumptions made. The electrostatic potential is then

$$U(\theta) = \frac{e}{C} \frac{h}{R_{\text{mach}}} \lambda(\theta) = \frac{g_0 eh}{4\pi\epsilon_0 R_{\text{mach}}} \lambda(\theta). \quad (4.11)$$

Therefore, in the non-relativistic approximation the longitudinal field strength is

$$E_\theta(\theta) = \frac{dU}{ds} = \frac{h}{R_{\text{mach}}} \frac{dU}{d\theta} = \frac{g_0 eh^2}{4\pi\epsilon_0 R_{\text{mach}}^2} \frac{d\lambda(\theta)}{d\theta}. \quad (4.12)$$

(Because of the sign conventions used, there is not the usual minus sign before the derivative.) Putting in the relativistic correction^{30,43} factor $1/\gamma^2$ we have

$$E_\kappa(\theta) = \frac{g_0 eh^2}{4\pi\epsilon_0 R_{\text{mach}}^2 \gamma_{\text{transition},0}^2} \frac{d\lambda(\theta)}{d\theta}. \quad (4.13)$$

We remark that we have used the value of γ at transition (the nominal transition, not modified by space-charge forces, as indicated by the subscript 0) also for energies which are only close to transition.

4.4 Transverse Space-Charge Forces⁴⁴

We assume that the transverse space-charge forces are linear as a function of the transverse coordinates, but we make no assumption on their dependence on the longitudinal coordinate θ . We can then use Laslett's theory.⁴⁵

From Laslett's paper we copy Eq. (8a):

$$N = B \frac{\pi b(a+b)}{2 r_p R} \times \frac{v_{y,0}^2 - v_y^2}{1 + \frac{b(a+b)}{h^2} [\epsilon_1(1 + B\beta^2\gamma^2) + \epsilon_2 B\beta^2\gamma^2(h^2/g^2)]} \times \beta^2\gamma^3. \quad (4.14)$$

Here, N is the number of particles in the machine associated with a shift in the number of vertical betatron oscillations per turn from $v_{y,0}$ to v_y . (We mean the individual-particle v -shift, and it is assumed that the centre of the beam remains at the centre of the vacuum chamber.) The beam has half-width a and half-height b , the vacuum chamber has half-height h , and the magnet poles have a half-distance g .

The classical particle radius is

$$r_p = \frac{e^2}{4\pi\epsilon_0 mc^2}, \quad (4.15)$$

and B is the bunching factor defined by

$$B = \frac{\text{average line-charge density}}{\text{peak line-charge density}}. \quad (4.16)$$

ϵ_1 is the electrostatic image coefficient and ϵ_2 is the magnetostatic image coefficient. Laslett⁴⁵ describes procedures by which ϵ_1 and ϵ_2 can be calculated. β and γ are the usual relativistic factors. R is the machine radius.

We have already used h to denote the harmonic number. Let us therefore rename the vacuum-chamber half-height and call it h_v . The magnet-pole half-distance we call g_m rather than g . We also replace R by R_{mach} , as πR^2 is often used to denote the bunch area. Let us also write Q_V instead of v_y . We introduce these minor changes of notation and at the same time we rewrite Laslett's formula in a form which is easier to discuss:

$$Q_V^2 - Q_{V,0}^2 = -N \frac{2}{\pi} r_p R_{\text{mach}} \times \left[\frac{1}{B\beta^2\gamma^3} \left(\frac{1}{b(a+b)} + \frac{\epsilon_1}{h_v^2} \right) + \frac{1}{\gamma} \left(\frac{\epsilon_1}{h_v^2} + \frac{\epsilon_2}{g_m^2} \right) \right]. \quad (4.17)$$

Written this way, the various "causes" (direct forces, image forces) appear on the right-hand side of the equation, the "effect" (Q -depression) appears on the left. The term

$$-N \frac{2}{\pi} r_p R_{\text{mach}} \frac{1}{B\beta^2\gamma^3} \frac{1}{b(a+b)} \quad (4.18)$$

represents the direct forces, the other terms represent the image forces.

Laslett's formula gives the vertical Q -shift, as this is the one that normally will limit the intensity. We are, however, interested in the horizontal Q -shift, as $v_{\text{transition}}$ is related to the horizontal Q . Let us therefore study the symmetry properties of the various terms.

For the direct fields we have

$$\nabla \cdot \mathbf{E}_{\text{direct}} \sim \rho, \quad \nabla \times \mathbf{B}_{\text{direct}} \sim \mathbf{j}, \quad (4.19)$$

the boundary conditions being those of free space. The rest of the fields are called image fields; for them the relations

$$\nabla \cdot \mathbf{E}_{\text{image}} = 0, \quad \nabla \times \mathbf{B}_{\text{image}} = 0 \quad (4.20)$$

must hold.

When modifying Eq. (4.17) to apply to the horizontal and not the vertical direction, for the direct fields we just interchange a and b . For the image fields it is a little more complicated.

Let us first consider the electric image fields. The contributions to the Q -depressions depend on the

force constants

$$\text{Force constant}_{el,H} = \frac{\partial E_x}{\partial x}, \quad (4.21)$$

$$\text{Force constant}_{el,V} = \frac{\partial E_y}{\partial y}. \quad (4.22)$$

Neglecting the longitudinal fields, which are usually small because of the geometry of the bunch, we have from Eq. (4.20):

$$\text{Force constant}_{el,H} = -\text{Force constant}_{el,V}. \quad (4.23)$$

Let us then turn to the magnetic image fields. The force constant in the horizontal direction is

$$\begin{aligned} \text{Force constant}_{mag,H} &= \frac{\partial}{\partial x} (\mathbf{v} \times \mathbf{B})_x \\ &= \frac{\partial}{\partial x} (v_y B_z - v_z B_y). \end{aligned} \quad (4.24)$$

Now v_y is small, and so is B_z , therefore we put

$$\text{Force constant}_{mag,H} = -v_z \frac{\partial B_y}{\partial x}. \quad (4.25)$$

For the vertical direction we find

$$\text{Force constant}_{mag,V} = v_z \frac{\partial B_x}{\partial y}. \quad (4.26)$$

Using now Eq. (4.20) we therefore find

$$\text{Force constant}_{mag,H} = -\text{Force constant}_{mag,V}. \quad (4.27)$$

So both electric and magnetic image terms just change their sign when we interchange the x - and y -directions, and we have from Eq. (4.17):

$$\begin{aligned} Q_H^2 - Q_{H,0}^2 &= -N \frac{2}{\pi} r_p R_{\text{mach}} \\ &\times \left[\frac{1}{B\beta^2\gamma^3} \left(\frac{1}{a(a+b)} - \frac{\varepsilon_1}{h_v^2} \right) - \frac{1}{\gamma} \left(\frac{\varepsilon_1}{h_v^2} + \frac{\varepsilon^2}{g_m^2} \right) \right]. \end{aligned} \quad (4.28)$$

An image term—say the term ε_1/h_v^2 —is a complicated function of geometry. As with the beam term, it happens to be possible to write it as

$$\frac{1}{\text{size}^2} \times \text{function (shape only)}. \quad (4.29)$$

It is just arbitrary that Laslett chose to use the vertical half-apertures h_v and g_m as his way of

describing the sizes. Therefore, there is nothing wrong in having h_v and g_m in image terms for the horizontal Q -depression. It has the advantage that ε_1 and ε_2 can be calculated by the methods of Laslett.⁴⁵

The particle number N in Laslett's formula is connected with our distribution function by the equation

$$N = h \int_{-\pi}^{\pi} \lambda(\theta) d\theta. \quad (4.30)$$

h denotes the harmonic number as before. Using the definition (4.16) for the bunching factor B , we have

$$B = \frac{N/(2\pi h)}{\lambda_{\max}}. \quad (4.31)$$

This is now substituted into Eq. (4.28) and we have

$$\begin{aligned} Q_H^2 - Q_{H,0}^2 &= -4hr_p R_{\text{mach}} \frac{1}{\beta^2\gamma^3} \left(\frac{1}{a(a+b)} - \frac{\varepsilon_1}{h_v^2} \right) \lambda_{\max} \\ &+ \frac{2}{\pi} r_p R_{\text{mach}} \frac{1}{\gamma} \left(\frac{\varepsilon_1}{h_v^2} + \frac{\varepsilon_2}{g_m^2} \right) N. \end{aligned} \quad (4.32)$$

We shall need not only the maximum Q -depression, but also the local Q -depression at θ . In analogy with Eq. (4.32) this must be

$$\begin{aligned} [Q_H(\theta)]^2 - Q_{H,0}^2 &= -4hr_p R_{\text{mach}} \frac{1}{\beta^2\gamma^3} \left(\frac{1}{a(a+b)} - \frac{\varepsilon_1}{h_v^2} \right) \lambda(\theta) \\ &+ \frac{2}{\pi} r_p R_{\text{mach}} \frac{1}{\gamma} \left(\frac{\varepsilon_1}{h_v^2} + \frac{\varepsilon_2}{g_m^2} \right) N. \end{aligned} \quad (4.33)$$

In an accelerator composed of sectors in all of which the radius of curvature is the same, separated by straight sections, we have according to Courant and Snyder³ that $\gamma_{\text{transition}} \approx Q_H$. The space-charge forces consist of magnetic as well as electric contributions; however, according to Hereward and Johnsen,⁴⁶ machines with electric focusing and machines with magnetic focusing have the same equations of motion in the transition range. We therefore put

$$\begin{aligned} [\gamma_{\text{transition}}(\theta)]^2 - (\gamma_{\text{transition},0})^2 &= -4hr_p R_{\text{mach}} \frac{1}{\beta^2\gamma^3} \left(\frac{1}{a(a+b)} - \frac{\varepsilon_1}{h_v^2} \right) \lambda(0) \\ &+ \frac{2}{\pi} r_p R_{\text{mach}} \frac{1}{\gamma} \left(\frac{\varepsilon_1}{h_v^2} + \frac{\varepsilon_2}{g_m^2} \right) N. \end{aligned} \quad (4.34)$$

This formula shows how the $\gamma_{\text{transition}}$ is modified by transverse space-charge forces. The transverse space-charge forces are assumed to be linear, so that they can be described by a force constant. This $\gamma_{\text{transition}}(\theta)$ will then be substituted into Eq. (4.4) to find the quantity η , which enters into the equation of motion (4.2).

4.5 $\gamma_{\text{transition}}\text{-jump}$

We take time t to be zero at the point where γ crosses $\gamma_{\text{transition},0}$. This common value of γ and $\gamma_{\text{transition},0}$ is denoted by $\gamma_{0,0}$. We allow $\gamma_{\text{transition},0}$ to be a function of time. In practice this can be arranged by pulsing a suitable set of quadrupole lenses in the machine, as discussed in Subsection 3.7. For more detailed discussions see other works.^{10,35,39,47-51} The difference between $\gamma_{\text{transition},0}$ and $\gamma_{0,0}$ will be denoted by $j(t)$ (j means "jump"). With our definitions $j(0) = 0$. This is

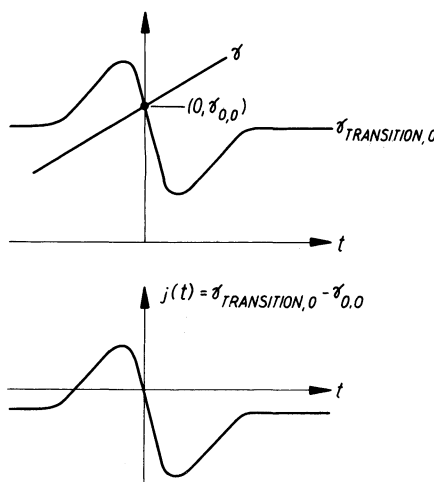


FIGURE 8 Notation.

illustrated in Figure 8. The transition "energy" neglecting space charge is

$$\gamma_{\text{transition},0} = \gamma_{0,0} + j(t) \quad (4.35)$$

and the "energy" of the synchronous particle is

$$\gamma = \gamma_{0,0} + \frac{eV \sin \phi_s}{mc^2} \frac{\beta_{0,0} c}{2\pi R_{\text{mach}}} t, \quad (4.36)$$

assuming a linear rise of γ with time. $\beta_{0,0}$ is defined by the equation

$$\gamma_{0,0} = (1 - \beta_{0,0}^2)^{-1/2}. \quad (4.37)$$

4.6 Nesting it All Together⁴⁴

On the right-hand side of Eq. (4.34) we replace all γ 's by $\gamma_{0,0}$ and β by $\beta_{0,0}$. Keeping only terms of the first order in t , $j(t)$, $\lambda(\theta)$, or N , we have by combining Eqs. (4.4), (4.34), (4.35) and (4.36):

$$\begin{aligned} \eta = & \frac{2}{\gamma_{0,0}^3} \frac{eV \sin \phi_s}{mc^2} \frac{\beta_{0,0} c}{2\pi R_{\text{mach}}} t - \frac{2}{\gamma_{0,0}^3} j(t) \\ & + 4hr_p R_{\text{mach}} \left(\frac{1}{a(a+b)} - \frac{\epsilon_1}{h_v^2} \frac{1}{\beta_{0,0}^2 \gamma_{0,0}^7} \right) \lambda(t, \theta) \\ & - \frac{2}{\pi} r_p R_{\text{mach}} \left(\frac{\epsilon_1}{h_v^2} + \frac{\epsilon_2}{g_m^2} \right) \frac{1}{\gamma_{0,0}^5} N. \end{aligned} \quad (4.38)$$

The fact that we have disregarded higher powers of t means that our theory is only valid in a limited range around transition, where η varies approximately linearly with t . (We could have avoided this approximation, but it makes life a little easier.) The theory is also not valid for very large excursions of $\gamma_{\text{transition},0}$ around $\gamma_{0,0}$. To remind ourselves that we shall have to take into account that the bunch length varies with time, we explicitly write $\lambda(t, \theta)$ and not only $\lambda(\theta)$ as we have done up to this point.

In the transition region η varies rapidly with time. This means that during one radian of the phase oscillation, η changes by a sizeable fraction of itself (it goes through zero). We can therefore take all the slowly-varying parameters in the equations of motion—like ω_s , β , E —to be constant without introducing any appreciable error. We take $\omega_s = \beta_{0,0} c / R_{\text{mach}}$, $\beta = \beta_{0,0}$ and $E = mc^2 \gamma_{0,0}$.

We shall now introduce scaled variables τ and p to replace t and ΔE (or $\Delta\gamma$). For simplicity, let us assume that ϕ_s is kept constant at all times t except at a few discrete times $t = t_1, t_2, \dots$, at which ϕ_s is instantaneously changed in such a way that $\sin \phi_s$ is kept constant and $\cos \phi_s$ gets the opposite sign to which it had before the phase switch. In other words, ϕ_s is say $\phi_s^{(1)}$ before the switch and $\phi_s^{(2)} = \pi - \phi_s^{(1)}$ after the switch. V is constant at all times. (This assumption simplifies the scaling but it is not necessary. A more general assumption is to let V and ϕ_s change simultaneously in such a way that $V \sin \phi_s$ is constant while permitting $V \cos \phi_s$ to be any function of time, see Subsection 9.5.) We substitute

$$t = T\tau \quad (4.39)$$

$$\Delta\gamma = \Gamma p, \quad (4.40)$$

and with the following choice of proportionality constants

$$T = \frac{R_{\text{mach}}}{c} \left\{ \frac{2\pi^2}{h} \left(\frac{mc^2}{eV} \right)^2 \frac{\gamma_{0,0}^4}{\beta_{0,0} \sin \phi_s |\cos \phi_s|} \right\}^{1/3} \quad (4.41)$$

$$\Gamma = \left\{ \frac{1}{4\pi h} \frac{eV}{mc^2} \frac{\beta_{0,0}^2 \gamma_{0,0}^4 \cos^2 \phi_s}{\sin \phi_s} \right\}^{1/3} \quad (4.42)$$

the equations of motion take the simple form

$$\frac{d}{d\tau} \theta = [\tau - \mu j(\tau) + \varepsilon \lambda(\tau, \theta) - \zeta N] p, \quad (4.43)$$

$$\frac{d}{d\tau} p = \frac{\sin(\phi_s + \theta) - \sin \phi_s}{|\cos \phi_s|} + \xi \frac{\partial \lambda(\tau, \theta)}{\partial \theta}, \quad (4.44)$$

with

$$\mu = \left\{ \frac{4h\pi}{\beta_{0,0}^2 \gamma_{0,0}^4} \frac{mc^2}{eV} \frac{|\cos \phi_s|}{\sin^2 \phi_s} \right\}^{1/3}, \quad (4.45)$$

$$\begin{aligned} \varepsilon = 4hr_p R_{\text{mach}} & \left(\frac{1}{a(a+b)} - \frac{\varepsilon_1}{h_v^2} \right) \\ & \times \left\{ \frac{h\pi}{2\beta_{0,0}^8 \gamma_{0,0}^{16}} \frac{mc^2}{eV} \frac{|\cos \phi_s|}{\sin^2 \phi_s} \right\}^{1/3}, \end{aligned} \quad (4.46)$$

$$\begin{aligned} \zeta = \frac{2}{\pi} r_p R_{\text{mach}} & \left(\frac{\varepsilon_1}{h_v^2} + \frac{\varepsilon_2}{g_m^2} \right) \\ & \times \left\{ \frac{h\pi}{2\beta_{0,0}^2 \gamma_{0,0}^{10}} \frac{mc^2}{eV} \frac{|\cos \phi_s|}{\sin^2 \phi_s} \right\}^{1/3}, \end{aligned} \quad (4.47)$$

$$\xi = \frac{2\pi h^2 g_0}{\gamma_{0,0}^2 |\cos \phi_s|} \frac{r_p}{R_{\text{mach}}} \frac{mc^2}{eV}. \quad (4.48)$$

The four parameters $\mu, \varepsilon, \zeta, \xi$ are all dimensionless: μ describes the sensitivity of the machine to a $\gamma_{\text{transition}}$ -jump, ε describes the sensitivity to the spread of $\gamma_{\text{transition}}$ due to transverse space-charge forces, and ζ is a proportionality factor for the dc shift of $\gamma_{\text{transition}}$. ξ describes the sensitivity to longitudinal space-charge forces.

The particle in question crosses transition when the bracket in Eq. (4.43) is zero. When ε and ζ are different from zero, this does not necessarily happen exactly at $\tau = 0$.

The scaling parameter T has the dimension of time. It is about 2 msec for the CERN PS and 1.6 msec for the CERN SPS. It is a measure of the duration of the nonadiabatic region around transition (provided we do not modify this by a $\gamma_{\text{transition}}$ -jump). The scaling parameter Γ is dimensionless.

Warning: the symbol p in Eqs. (4.40), (4.43), (4.44) does not denote $mc\beta\gamma$. It is the canonical conjugate to the phase ϕ .

5 EQUATION OF MOTION FOR THE BUNCH (VLASOV EQUATION)

The equations of motion (4.43), (4.44) describe how a particle moves about in the (ϕ, p) space. If we know how every single particle in the bunch moves, it must be possible to describe the motion of the bunch as a whole. This can be done by transforming the single-particle equations into a Vlasov equation⁴⁴ (collisionless Boltzmann equation). The Vlasov equation is a partial differential equation describing the motion of the phase-space density of particles $\rho(t, \phi, p)$.

The density $\rho(t, \phi, p)$ will move like an incompressible fluid and will therefore follow the differential equation

$$\frac{\partial \rho}{\partial \tau} = - \left(\frac{\partial \rho}{\partial \phi} \frac{d\phi}{d\tau} + \frac{\partial \rho}{\partial p} \frac{dp}{d\tau} \right), \quad (5.1)$$

see Figure 9. Using the single-particle equations (4.43), (4.44), we have the equation of motion for the density ρ :

$$\begin{aligned} \frac{\partial \rho}{\partial \tau} = - & [(\tau - \mu j(\tau) + \varepsilon \lambda(\tau, \theta) - \zeta N) p \frac{\partial \rho}{\partial \theta} \\ & - \left(\frac{\sin(\phi_s + \theta) - \sin \phi_s}{|\cos \phi_s|} + \xi \frac{\partial \lambda(\tau, \theta)}{\partial \theta} \right) \frac{\partial \rho}{\partial p}]. \end{aligned} \quad (5.2)$$

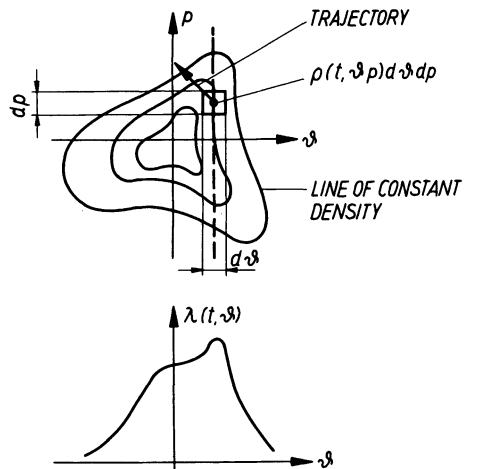


FIGURE 9 Motion of the phase-space density.

$\lambda(\tau, \theta)$ denotes the number of particles per rf radian, not bothering about their energies. λ is therefore related to ρ by the equation

$$\lambda(\tau, \theta) = \int_{-\infty}^{\infty} \rho(\tau, \theta, p) dp. \quad (5.3)$$

N denotes the number of particles in the machine. Assuming all bunches equal, this is given by

$$N = h \int_{-\pi}^{\pi} \lambda(\tau, \theta) d\theta. \quad (5.4)$$

6 ELLIPSE DESCRIPTION OF THE BUNCH MOTION⁸

6.1 What such a Simple Description Can Give Us

The solution of the Vlasov equation—Eq. (5.2)—gives a complete description of the motion of the bunch. But solving the Vlasov equation is a heavy exercise, and some insight into the problem can be gained from a simplified approximate description of the motion of the bunch. Such a simplified theory does not give all the physics of a real accelerator, but it is more convenient to use and is often sufficient. Most of the theoretical work existing today is based on the ellipse description of the bunch.

Suppose we have an elliptic bunch. By this we shall mean that all equidensity contours, $\rho(\theta, p) = \text{constant}$, are ellipses with the same shape and tilt. We do not permit general shapes as shown in Figure 9. Will such an elliptic bunch stay elliptic for ever? No, not in general. But if the single-particle equations of motion are linear in θ and p , the phase space will undergo only linear transformations. Now, a linear transformation of an ellipse is simply a new ellipse, and the bunch will therefore stay elliptic.

Let us therefore take a close look at the various terms of Eqs. (4.43) and (4.44) to find out which are linear and which are not. The linear ones we keep as they are, the nonlinear ones we shall either linearize or throw away. With this approximation it will be possible to describe the bunch in terms of an ellipse. As an ellipse can be completely defined by only three parameters, for instance area, eccentricity and tilt, we arrive at a very simple description of the motion of the bunch. In our case, the area of the ellipse even turns out to be constant, and the bunch is therefore described by only two parameters. These two parameters, which we

denote Θ and P , have almost the same equations of motion as the single-particle quantities θ and p .

This simplicity we pay for by a loss of accuracy. Not all sorts of accuracy are lost to the same degree. The observed emittance growth is a phenomenon which is nonlinear in an essential way: our ellipse description yields ellipse with constant area. The ellipse description will therefore not give us any insight into the mechanisms that cause the emittance growth. On the other hand, the ellipse description correctly tells us that the bunch length has a narrow minimum at transition, and that bunch-length oscillations occur after transition. The amplitude and phase of these oscillations are correctly given,⁸ as well as the rapidity with which the oscillations start,⁸ and their response to manipulations with the machine like the $\gamma_{\text{transition}}$ -jump.⁹

Insight into the mechanisms causing emittance blow-up can be gained from more refined, nonlinear calculations. These calculations are carried out on a computer and consume a fair amount of computer time for every case investigated. Therefore only a limited number of cases can be investigated that way. But once such insight exists, results of the linear theory can sometimes be improved by qualitative arguments like the following: "As the linear theory predicts a very small momentum spread, this case will only have very little Landau damping and the negative-mass instability will produce a large emittance blow-up." Although more accurate calculation methods do exist, it is still valuable to have a quick-and-dirty method by which one can rapidly investigate a number of different cases. We shall come back to these more accurate methods in Sections 7, 8 and 9.

Let us also remark here that one of these more accurate methods uses the ellipse formulation as its starting point.

6.2 Linearization of the Single-Particle Equations

Let us now discuss term after term of the equations of motion for a single particle, Eqs. (4.43) and (4.44).

Take first the rf focusing term

$$[\sin(\phi_s + \theta) - \sin \phi_s]/[\cos \phi_s].$$

If the particles are tightly bunched around the phase-stable point so that θ is small for all particles, we can to a good approximation linearize this to $\text{sgn}(\cos \phi_s)\theta$. [The function $\text{sgn}(x)$ is equal to $+1$ if $x > 0$ and equal to -1 if $x < 0$]. At transition the bunches are normally very short, so this

approximation is quite good. But we cannot study how particles are lost out of the bucket if the final distortion of the bunch is very large, as the existence of a finite bucket is due to the nonlinearity of the rf forces. Also filamentation cannot be studied in this approximation.

Let us then investigate the longitudinal space-charge forces $\zeta \partial\lambda(\tau, \theta)/\partial\theta$. In general $\lambda(\theta)$ may have any shape. In the CERN PS, where the high-frequency beam observation equipment has permitted an extensive experimental study of bunch shapes, it has been found that before transition the bunches are roughly of parabolic shape, or perhaps somewhat sharper at the peak.^{4,52} At lower beam intensities the same is true after transition, while at high intensities the bunches often develop strange shapes after transition, for instance they sometimes get two peaks, see Figure 2. If the emittance blow-up is actually due to the negative-mass instability, as is believed,^{11,12} there is probably a complicated short-wavelength structure on top of what is observable, as theoretical arguments³⁰ indicate that the negative-mass instability has the highest growth rate at very short wavelengths. In fact, the fastest-growing mode has a wavelength comparable to the kernel width d/γ or about 1 cm in the CERN PS, see Subsection 4.3. Let us, however, neglect all these complications and assume that the bunch has exactly the shape of a segment of a parabola, so that $\partial\lambda/\partial\theta$ becomes linear everywhere where there are particles, as illustrated in Figure 10. Where there are no particles to "observe" the

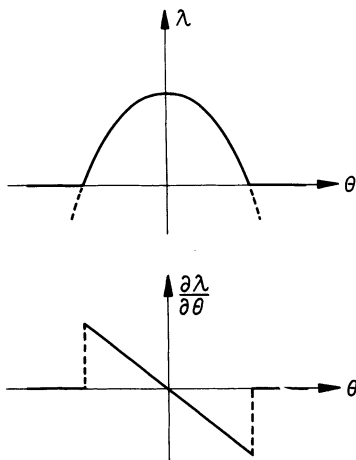


FIGURE 10 Bunch shape giving linear longitudinal space-charge forces.

field, it does not matter what is the shape of the field.

Let us denote the bunch half-length by $\hat{\theta}$. Our task will be to derive a differential equation for $\hat{\theta}$, and for another quantity which is the canonical conjugate to $\hat{\theta}$. This will give us a description of the motion of the bunch as a whole. Assume that the bunch is centred around the stable phase angle (this is not always the case). A parabolic bunch shape is then given by

$$\lambda(\theta) = \begin{cases} \frac{3}{4} \frac{N}{h\hat{\theta}} \left[1 - \left(\frac{\theta}{\hat{\theta}} \right)^2 \right] & \text{for } |\theta| \leq \hat{\theta} \\ 0 & \text{for } |\theta| \geq \hat{\theta}. \end{cases} \quad (6.1)$$

Taking the derivative we have

$$\xi \frac{\partial\lambda(\theta)}{\partial\theta} = -\frac{3}{2} \xi \frac{N}{h\hat{\theta}^3} \theta \quad \text{for } |\theta| < \hat{\theta}. \quad (6.2)$$

A parabolic shape of $\lambda(\theta)$ implies that in phase space the density $\rho(\theta, p)$ is decreasing when going from the centre to the edge of the bunch. For an elliptic bunch in principal axes with half-axes $\hat{\theta}$ and \hat{p} the density is⁵³

$$\rho(\theta, p) = \frac{3}{2h} \frac{N}{\pi\hat{\theta}\hat{p}} \left[1 - \left(\frac{\theta}{\hat{\theta}} \right)^2 - \left(\frac{p}{\hat{p}} \right)^2 \right]^{1/2} \quad \text{for } \left(\frac{\theta}{\hat{\theta}} \right)^2 + \left(\frac{p}{\hat{p}} \right)^2 \leq 1. \quad (6.3)$$

We have now linearized the equation of motion for p , Eq. (4.44); we go on with the equation of motion for θ . The term τp describing the ordinary crossing of transition is linear as it is, the same is true with the term $-\mu j(\tau)p$ describing the effect of a $\gamma_{\text{transition}}$ -jump, so we have no worries here.

The term $\varepsilon\lambda(\tau, \theta)p$ describing the spreading-out of $\gamma_{\text{transition}}$ due to transverse space-charge forces is a little more complicated. It can be split into two parts, a part proportional to p and another part proportional to $\theta^2 p$. The first part means a shift of the transition energy, the shift being the same for all particles. We can easily handle this term, but as its effect is not very interesting (it will just shift the optimal timings by a small amount), we shall drop it anyway. The last term is a genuine nonlinear term which we cannot handle with an ellipse formalism.

The term $-\zeta N p$ also describes a shift of transition energy that is the same for all particles. As it is linear, we can handle it with an ellipse formalism, but again its effect is not very interesting. It is

also very small in most machines, because it consists entirely of image forces: if the image coefficients ε_1 and ε_2 of Laslett are equal to zero, ζ is also zero, as can be seen from Eq. (4.47). The ellipse formalism is only approximate anyway, and it is not worth the trouble to include this term.

With these simplifications the single-particle equations of motion take this form:

$$\frac{d}{d\tau} \theta = [\tau - \mu j(\tau)] p \quad (6.4)$$

$$\frac{d}{d\tau} p = \operatorname{sgn}(\cos \phi_s) \theta - \frac{3}{2} \frac{N}{h\hat{\theta}^3} \xi \theta. \quad (6.5)$$

Looking back to the list of mechanisms and cures listed in Section 4.1, these equations contain the points (1a), (7) and (8).

If the single particles follow these linear equations of motion, an elliptic bunch will stay elliptic forever. We shall now derive an equation of motion for the bunch as a whole.

6.3 Equations of Motion for an Elliptic Bunch

Suppose the two-single-particle variables θ and p are connected by linear first-order differential equations. The most general form of such equations is

$$\frac{d}{d\tau} \begin{pmatrix} \theta \\ p \end{pmatrix} = \begin{pmatrix} F_1 & F_2 \\ F_3 & F_4 \end{pmatrix} \begin{pmatrix} \theta \\ p \end{pmatrix}. \quad (6.6)$$

The F 's may be functions of the independent variable τ , they may also be functions of quantities like $\hat{\theta}$, $\langle \theta^2 \rangle$, $\langle p^2 \rangle$, which describe the bunch as a whole. But the F 's must be the same for every particle; if they depended in any way on θ or p of the individual particle the equations would not be linear. Clearly Eqs. (6.4), (6.5) belong to this general class, with

$$\left. \begin{array}{l} F_1 = 0, \\ F_2 = \tau - \mu j(\tau), \\ F_3 = \operatorname{sgn}(\cos \phi_s) - \frac{3}{2} \xi \frac{N}{h\hat{\theta}^3}, \\ F_4 = 0. \end{array} \right\} \quad (6.7)$$

The mapping of coordinate and momentum of a particle from $\tau = \tau_1$ to $\tau = \tau_2$ is then also governed by a linear relationship

$$\begin{pmatrix} \theta \\ p \end{pmatrix}_{\tau_2} = \begin{pmatrix} T_1 & T_2 \\ T_3 & T_4 \end{pmatrix}_{\tau_1 \rightarrow \tau_2} \begin{pmatrix} \theta \\ p \end{pmatrix}_{\tau_1} \quad (6.8)$$

or in shorthand

$$\theta_{\tau_2} = T_{\tau_1 \rightarrow \tau_2} \theta_{\tau_1}. \quad (6.9)$$

Since we know the motion of the individual particles, we can determine the evolution of any distribution of particles in phase space.

We specify the boundary ellipse by the quadratic form

$$(\theta, p) \begin{pmatrix} M_1 & M_2 \\ M_2 & M_4 \end{pmatrix}_{\tau}^{-1} \begin{pmatrix} \theta \\ p \end{pmatrix} = 1 \quad (6.10)$$

or in shorthand

$$\tilde{\theta} M_{\tau}^{-1} \theta = 1. \quad (6.11)$$

From Liouville's theorem we know that a particle which is at the boundary at $\tau = \tau_1$ will also be at the new boundary ellipse at $\tau = \tau_2$. Its coordinate and momentum will therefore satisfy Eq. (6.11) at τ_1 and τ_2 :

$$\tilde{\theta}_{\tau_1} M_{\tau_1}^{-1} \theta_{\tau_1} = 1 \quad (6.12)$$

$$\tilde{\theta}_{\tau_2} M_{\tau_2}^{-1} \theta_{\tau_2} = 1. \quad (6.13)$$

Substituting Eq. (6.9) into Eq. (6.13) we have

$$\tilde{\theta}_{\tau_1} (\tilde{T}_{\tau_1 \rightarrow \tau_2} M_{\tau_2}^{-1} T_{\tau_1 \rightarrow \tau_2}) \theta_{\tau_1} = 1. \quad (6.14)$$

Equations (6.12) and (6.14) must be satisfied for any particle lying on the boundary at $\tau = \tau_1$, not only for a particular one. This means that

$$M_{\tau_1}^{-1} = \tilde{T}_{\tau_1 \rightarrow \tau_2} M_{\tau_2}^{-1} T_{\tau_1 \rightarrow \tau_2} \quad (6.15)$$

or

$$M_{\tau_2} = T_{\tau_1 \rightarrow \tau_2} M_{\tau_1} \tilde{T}_{\tau_1 \rightarrow \tau_2}. \quad (6.16)$$

If the infinitesimal form $T = I + F d\tau$ is used in Eq. (6.16), we find the differential equation

$$\frac{dM}{d\tau} = FM + MF \quad (6.17)$$

or written out in full

$$\left. \begin{array}{l} \frac{dM_1}{d\tau} = 2(F_1 M_1 + F_2 M_2) \\ \frac{dM_2}{d\tau} = F_3 M_1 + (F_1 + F_4) M_2 + F_2 M_4 \\ \frac{dM_4}{d\tau} = 2(F_3 M_2 + F_4 M_4). \end{array} \right\} \quad (6.18)$$

We have now established equations of motion† for the three quantities M_1 , M_2 , M_4 in terms of

† These equations were first derived in Ref. 8. The shorter derivation given here is due to F. Sacherer.⁵⁴

which we describe the ellipse, Eq (6.10). However, Eqs. (6.18) are not particularly easy to work with. Let us therefore introduce three new variables R , Θ , P , whose equations of motion are easier to work with. We put

$$\left. \begin{aligned} R &= (M_1 M_4 - M_2^2)^{1/4} \\ \Theta &= M_1^{1/2}/(M_1 M_4 - M_2^2)^{1/4} \\ P &= M_2/[M_1^{1/2}(M_1 M_4 - M_2^2)^{1/4}], \end{aligned} \right\} \quad (6.19)$$

or inversely

$$\left. \begin{aligned} M_1 &= R^2 \Theta^2 \\ M_2 &= R^2 \Theta P \\ M_4 &= R^2 (P^2 + 1/\Theta^2). \end{aligned} \right\} \quad (6.20)$$

The equations of motion for R , Θ , P are

$$\left. \begin{aligned} \frac{dR}{d\tau} &= \frac{1}{2}(F_1 + F_4)R \\ \frac{d\Theta}{d\tau} &= \frac{1}{2}(F_1 - F_4)\Theta + F_2 P \\ \frac{dP}{d\tau} &= F_3 \Theta - \frac{1}{2}(F_1 - F_4)P + F_2/\Theta^3 \end{aligned} \right\} \quad (6.21)$$

At first sight these equations do not appear to be much simpler than Eqs. (6.18). They have, however, the important advantage that R is completely decoupled from Θ and P . If, moreover, the original equations of motion (6.6) are canonical, then $F_1 + F_4 = 0$ and we have $dR/d\tau = 0$. Then R is a constant of motion, and Eqs. (6.21) effectively degenerate into only two equations, as the solution for R is trivial.

With $F_1 + F_4 = 0$ the equations of motion for Θ and P are the same as those for θ and p , except for the extra term F_2/Θ^3 . A similar term appears in the equations for the transverse bunch dimensions.⁵⁵

Up to this point we have treated the problem of two linear single-particle equations in a general way. Let us now go back to our specific equations, substituting the F 's given by Eqs. (6.7):

$$\left. \begin{aligned} \frac{dR}{d\tau} &= 0 \\ \frac{d\Theta}{d\tau} &= [\tau - \mu j(\tau)]P \\ \frac{dP}{d\tau} &= \left[\operatorname{sgn}(\cos \phi s) - \frac{3}{2} \xi \frac{N}{h \hat{\theta}^3} \right] \Theta + \frac{\tau - \mu j(\tau)}{\Theta^3}. \end{aligned} \right\} \quad (6.22)$$

6.4 Interpretation of the Bunch Variables

Combining Eqs. (6.10) and (6.20) we have the following equation for the ellipse:

$$(P^2 + 1/\Theta^2)\theta^2 - 2\Theta P \theta p + \Theta^2 p^2 = R^2. \quad (6.23)$$

This ellipse can also be described parametrically as

$$\left(\begin{array}{c} \theta \\ p \end{array} \right) = \left(\begin{array}{cc} R\Theta & 0 \\ RP & R/\Theta \end{array} \right) \left(\begin{array}{c} \cos \Psi \\ \sin \Psi \end{array} \right), \quad (6.24)$$

where Ψ runs through all numbers between 0 and 2π .

From these equations we find:

$$\left. \begin{aligned} \text{Ellipse area} &= E = \pi R^2 \\ \text{Ellipse half-length} &= \hat{\theta} = R\Theta \\ \text{Half-height between end points} &= H = RP. \end{aligned} \right\} \quad (6.25)$$

These relations are illustrated by Figure 11. These three relations are sufficient to determine R , Θ , P of a given ellipse. They are also sufficient to determine the ellipse from given values of R , Θ , P .

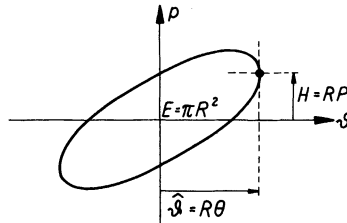


FIGURE 11 The physical meaning of the ellipse variables R , Θ , P .

The following four relations may also be useful:

$$\left. \begin{aligned} \text{Ellipse half-height} &= \hat{p} = R(P^2 + 1/\Theta^2)^{1/2} \\ \text{Half-length between peak points} &= L = R\Theta P / (P^2 + 1/\Theta^2)^{1/2} \\ \text{Ellipse cuts } \theta\text{-axis at} & \quad \theta = R/(P^2 + 1/\Theta^2)^{1/2} \\ \text{Ellipse cuts } p\text{-axis at} & \quad p = R/\Theta. \end{aligned} \right\} \quad (6.26)$$

These latter relations are illustrated in Figures 12 and 13.

6.5 Connection between the two Space-Charge Parameters N_0 and $\eta_0(0)$

In the equation of motion for P , Eq. (6.22), appears the quantity $\hat{\theta}$ which denotes the ellipse half-

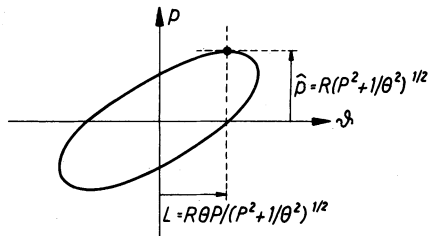


FIGURE 12 Position of the point of maximum height.

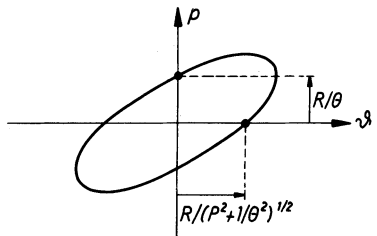


FIGURE 13 Position of the points where the ellipse crosses the axes.

length. Using Eqs. (6.25) we can eliminate this quantity. It is useful to introduce the space-charge parameter

$$N_0 = \frac{3}{2} \frac{\xi N}{hR^3}, \quad (6.27)$$

which gives

$$\left. \begin{aligned} \frac{dR}{d\tau} &= 0 \\ \frac{d\Theta}{d\tau} &= [\tau - \mu j(\tau)]P \\ \frac{dP}{d\tau} &= \text{sgn}(\cos \phi_s)\Theta - \frac{N_0}{\Theta^2} + \frac{\tau - \mu j(\tau)}{\Theta^3} \end{aligned} \right\} \quad (6.28)$$

If we do not manipulate the machine by the $\gamma_{\text{transition}}\text{-jump}$ or phase jumps [expressed through the terms $-\mu j(\tau)$ and $\text{sgn}(\cos \phi_s)$, respectively] the whole development of the bunch as a function of time depends on the single parameter N_0 .

Our definition of the space-charge parameter N_0 involves a quantity R . This R is given by requiring that πR^2 shall be the bunch area in units of $\Delta\phi \times \Delta p$. (Note p is the conjugate momentum to ϕ and is not equal to $mc\beta\gamma$.) It is useful to have a formula giving N in terms of more physical units. Let A denote the bunch area in units of $\Delta(\phi_{\text{rf}}) \times \Delta(\beta\gamma)$. N_0 is then given by

$$N_0 = \frac{3\pi^2}{2} Ng_0 \frac{r_p}{R} \left(\frac{mc^2}{eV} \frac{h}{\beta \sin \phi_s} \right)^{1/2} \frac{1}{A^{3/2}}. \quad (6.29)$$

In addition to the space-charge parameter N_0 which we have defined through Eqs. (6.27) and (4.48), another parameter denoted by $\eta_0(0)$ is also frequently used in the literature.²⁸ Let $\eta_{\text{sp-ch}}(\tau)$ denote the ratio of longitudinal space-charge forces to the focusing component of the rf forces. As the bunch length changes, this ratio is evidently a function of the scaled time τ . We may evaluate this ratio approximately, neglecting the influence of space-charge forces on the bunch shape. This approximation we denote by $\eta_0(\tau)$. Its value at the moment when transition is crossed is $\eta_0(0)$. This quantity can be taken as a measure of the importance of the longitudinal space-charge forces. $\eta_0(0)$ has the advantage that it can be defined in physical terms; N_0 has the advantage that it is the quantity that appears directly in the equations of motion.

Even in the absence of space charge the equations of motion for Θ and P are nonlinear. But without space charge the single particles do not couple to each other, and the single-particle equations can be solved without already knowing $\hat{\theta}$. The single-particle equations can then be solved analytically. Knowing two single-particle solutions, we also know the motion of the bunch as a whole.⁸ In this way one can establish analytical solutions for Θ and P . In fact, Θ and P are just nonlinear functions of solutions of linear differential equations. We give here the solution in the absence of space charge and $\gamma_{\text{transition}}\text{-jump}$ and with one phase switch exactly at transition. The solution is expressed in terms of Bessel functions and Neumann functions of order 2/3. With the abbreviations

$$J = J_{2/3}(\frac{2}{3}|\tau|^{3/2}), \quad N = N_{2/3}(\frac{2}{3}|\tau|^{3/2}), \quad (6.30)$$

Θ is given by

$$\Theta = |\tau| \left(\frac{\pi}{3} \right)^{1/2} [(u^2 \cos^2 v + u^{-2} \sin^2 v) J^2 - 2 \cos v \sin v (u^2 - u^{-2}) J N + (u^2 \sin^2 v + u^{-2} \cos^2 v) N^2]^{1/2}, \quad (6.31)$$

where u and v are arbitrary constants.

In the presence of space charge, $N_0 \neq 0$, an analytical solution is not known.

Assuming that well before transition the bunch does not oscillate, we must take $u = 1$, which implies that at transition

$$\Theta(0) = \frac{3^{1/6}}{\pi^{1/2}} \Gamma\left(\frac{2}{3}\right) \approx 0.9175. \quad (6.32)$$

This gives the following relation:

$$N_0 = \frac{3^{1/2}}{\pi^{3/2}} \left[\Gamma\left(\frac{2}{3}\right) \right]^3 \eta_0(0) \approx 0.7723 \eta_0(0). \quad (6.33)$$

6.6 Hamiltonian Formulation of the Bunch Equations

The equations of motion for Θ and P can be derived from the Hamiltonian

$$\begin{aligned} H(\tau, \Theta, P) = & \frac{1}{2} [\tau - \mu j(\tau)] P^2 - \frac{1}{2} \operatorname{sgn}(\cos \phi_s) \Theta^2 \\ & - \frac{N_0}{\Theta} + \frac{1}{2} \frac{\tau - \mu j(\tau)}{\Theta^2}. \end{aligned} \quad (6.34)$$

This Hamiltonian has not much to do with an energy: it only has the property that the equations of motion for Θ and P can be derived from it as Hamilton's equations:

$$\left. \begin{aligned} \frac{d\Theta}{d\tau} &= \frac{\partial H}{\partial P} = [\tau - \mu j(\tau)] P \\ \frac{dP}{d\tau} &= -\frac{\partial H}{\partial \Theta} \\ &= \operatorname{sgn}(\cos \phi_s) \Theta - \frac{N_0}{\Theta^2} + \frac{\tau - \mu j(\tau)}{\Theta^3} \end{aligned} \right\} \quad (6.35)$$

This proves that Θ and P are canonically conjugate to each other.

Besides its formal properties, such a Hamiltonian is sometimes a useful computational tool, because it is a semi-invariant of the motion. As time (or rather the scaled time, τ) enters explicitly into the Hamiltonian, we cannot expect it to be invariant, but we find

$$\begin{aligned} \frac{dH}{d\tau} &= \frac{1}{2} \left(P^2 + \frac{1}{\Theta^2} \right) \left[1 - \mu \frac{dj(\tau)}{d\tau} \right] \\ &= \frac{1}{2} \left(\frac{\tilde{p}}{R} \right)^2 \left[1 - \mu \frac{dj(\tau)}{d\tau} \right]. \end{aligned} \quad (6.36)$$

As the sign of $dH/d\tau$ is independent of Θ and P , H cannot oscillate up and down as do Θ and P . For reasonably short intervals of time one may put $H(\tau, \Theta, P)$ equal to a constant, and in this way one has an approximation to a phase trajectory without having to integrate numerically the equations of motion.

6.7 Numerical Calculations

The ellipse equations (6.28) have been the basis of many theoretical papers. First the bunch-length oscillations caused by longitudinal space-charge forces in an uncorrected machine were analysed this way.⁸ These calculations reproduce experiments quite well as far as the oscillations go, but they do not at all account for the emittance blow-up. Then a machine working with heavy space charge but corrected by triple switch was analysed.⁸ These calculations agree less well with experiments due to the enhanced negative-mass instability, see Section 7. Finally there followed a long series of papers^{9,35-40} on the $\gamma_{\text{transition}}$ -jump. The $\gamma_{\text{transition}}$ -jump was invented to cure the bunch-length oscillations, but most versions of it help against the instability as well. (An upward jump is an exception.) Therefore, most of these calculations agree quite well with experiments.¹⁰ As we have now some insight into how the negative-mass instability works, we can by qualitative arguments predict whether a given calculation will give correct results or not.

For the $\gamma_{\text{transition}}$ -jump many different waveforms have been investigated, with different jump magnitudes and jump speeds. It would be too long to summarize all these results here. Let us just mention that complete suppression of the oscillations for a given space-charge parameter is not the only goal. With some versions of the $\gamma_{\text{transition}}$ -jump the final amount of oscillation is very insensitive to variations of the space-charge parameter around its nominal value. With other versions a small deviation from the nominal value, either up or down, produces a large amount of oscillation. Generally, the larger the jump, and the greater its speed, the less sensitive is the machine to intensity fluctuations.^{9,50} One may assume that this also means that nonlinearities of the space-charge force are less important, as nonlinearities can be understood as different particles having different space-charge parameters.

In some machines like the CERN SPS, the aperture limitation is not at injection, but at transition due to the large momentum spread. In order to reduce this momentum spread, the possibility of switching the rf phase back and forth many times,⁵⁶ so as to keep the bunches long and slender has been investigated. Using seven phase switches instead of one, the maximum momentum spread can be reduced by a factor of 0.74. As the

CERN SPS has very little space charge,¹⁴ this number is probably rather reliable.

7 SUPER-PARTICLE DESCRIPTION OF THE BUNCH MOTION

7.1 *The Super-Particle Method*

In Section 6 we had to work with linearized single-particle equations of motion in order to be able to describe the bunch motion in terms of an ellipse. When linearizing the equations we lose some of the physics, as discussed in Subsections 6.1 and 6.2. In this section we shall bring some of this physics back in. We use the full equations (4.43), (4.44) as our starting point. As we do not linearize the equations, the simple and convenient ellipse description of the bunch has unfortunately to be abandoned. In this section we discuss some calculations^{11,15} done with the super-particle method⁵⁷; in the next section (Section 8) we present the results of some calculations¹² with a method in which the phase-space density ρ is expanded into Hermite polynomials.^{58,59}

Subsection 7.2 deals with super-particle calculations on the influence of longitudinal space-charge forces.¹¹ As short wavelengths as possible are taken into account to be able to simulate the negative-mass instability, at least to some degree. Subsection 7.3 deals with the influence of transverse space-charge forces on the longitudinal motion.¹⁵ This is not a short-wavelength phenomenon, and short wavelengths are excluded from the calculations to increase their speed. Although the super-particle method is very flexible and could easily be made to handle the negative-mass instability and the transverse effect simultaneously, such a combined calculation has not been done. Probably the two mechanisms would just add their effects.

The super-particle method consists essentially of replacing N actual particles by a smaller number n of "super-particles." If the actual particles have mass m and charge q , the "super-particles" have mass $(N/n)m$ and charge $(N/n)q$ so that the total mass and total charge are the same in the actual system and in the simulated system. For a bunch in an accelerator the number of particles is typically in the range 10^{11} to 10^{12} . The number of super-particles is an economical problem, 10^3 is a typical value. The super-particle method will over-emphasize two-body collisions because of the increased "granularity" of matter. A super-particle has a

smaller number of companions than an actual particle, but this is more than compensated by the fact that the cross section is proportional to the square of the charge. Various techniques⁵⁷ exist to reduce the effects of two-body collisions in the calculation. These techniques amount to treating small particle distances in some special way, modifying the force law.

7.2 *Longitudinal Space-Charge Forces and the Negative-Mass Instability*

This study has been carried out by Lee and Teng.¹¹ We shall discuss their findings here.

In Eq. (4.43) they dropped the terms $\varepsilon\lambda(\tau, \theta)p$ and $-\zeta Np$ describing the influence of transverse space-charge forces. On the other hand, they used a somewhat more general equation of motion for p than Eq. (4.44), in that they permit any variation of the stable phase angle ϕ_s with time. [Equation (4.44) only permits the values $\phi_s^{(1)}$ and $\phi_s^{(2)} = \pi - \phi_s^{(1)}$ with an infinitely fast switch between them. Compare also with Subsection 9.5.] The characteristic time T does then not have a clear meaning any more, and the scaling of the equations has to be done in a somewhat different way.

The space-charge force is given by the derivative of the line-charge density, $\xi \partial\lambda(\tau, \theta)/\partial\theta$. To work out this numerically they divided the θ -axis into bins of equal widths and counted up how many particles there were in each bin. The space-charge force on a particle in the k th bin was then determined by the difference between the number of particles in bin $k - 1$ and the number of particles in bin $k + 1$.

In addition to the familiar bunch-length oscillations they observed a negative-mass instability that develops right after transition. The bunch breaks up into a number of irregular small lumps, causing an increase of the longitudinal emittance. This observation is so important that their paper marks a turning-point in the understanding of transition phenomena.

The history of the negative-mass instability as an explanation of the blow-up is quite interesting. In a paper at the 1967 International Accelerator Conference, Lebedev⁶⁰ derived an equation which implies that, in a bunched beam, there will be no negative-mass instability if the bunches are matched to the buckets. Lebedev did not formulate his equation in words, and one tended to forget the condition about matching. The important point is that right after transition the bunch is much longer

and has much less energy spread than it would have in a matched condition.

Theoretical arguments indicate that the fastest-growing modes have a wavelength which is of the order d/γ , as mentioned in Subsection 6.2. (The factor γ is forgotten in Ref. 11.) The bin width should therefore be of about the same size if the force is calculated by the simple difference between bin counts just described. Preferably, the bins should be even narrower than this and the electric field be calculated from a finite kernel, such as the one given by Eq. (4.7). On the other hand, there has to be a sufficiently large number of super-particles per bin to avoid too large statistical fluctuations. The statistical fluctuations are, of course, aggravated as one takes the difference between two counts. As the total number of super-particles is limited, for economic reasons, the bins must therefore not be made too narrow. When choosing bin width one has to strike a delicate balance: too wide bins will smear out all short-wavelength phenomena, while too narrow bins will result in too large statistical fluctuations. This balance depends on how many super-particles one can afford to use. Lee and Teng¹¹ used 2000 super-particles distributed over 10 to 20 bins. At the end of the run, after the instability had taken place, the dominant perturbation always had a wavelength about equal to the bin width. As the bunches are about 2.5 m long and d/γ is about 1 cm in their machine, they should ideally have used at least 250 bins, preferably more. A correspondingly large number of super-particles would not be economically feasible. This means that one must not believe the details of their calculation, although it certainly gives us a lot of physical insight into the negative-mass instability. A detailed calculation would be very difficult to carry out. As they miss the fastest-growing modes, the actual instability is probably worse than the simulated one.

They also performed some runs to simulate various cures and made the following observations.

Triple switch,^{22,23} which in the linear approximation⁸ (ellipse theory) appears as a very good cure for bunch-length oscillations, turns out to make the negative-mass instability much worse. The rf defocusing keeps the bunch long, with low energy-spread. The Landau damping is thereby reduced and the negative-mass instability can act unhindered. A method called the double switch¹¹ [in which ϕ_s is first jumped from $\phi_s^{(1)}$ to some intermediary value $\phi_s^{(2)}$ and then to $\phi_s^{(3)} = \pi - \phi_s^{(1)}$] has essentially the same properties: it cures oscil-

lations but aggravates the instability.

Various versions of the $\gamma_{\text{transition}}$ -jump did much better. The smallest influence of the negative-mass instability was observed with a rapid downward jump of $\gamma_{\text{transition}}$, despite the fact that the energy spread is kept small with this scheme. The reason is that due to the rapid downward jump of $\gamma_{\text{transition}}$ very little time is spent in the dangerous regime close to transition where η is small. Upward jumps of $\gamma_{\text{transition}}$ were more subject to the instability.

Lee and Teng compared their numerical results with a generalized version of the criterion for the negative-mass instability given by Neil and Sessler.³⁰ Neil and Sessler have found that an unbunched beam is stable if

$$(\Delta\gamma)^2 > \frac{4\beta^2 g_0 r_p}{\gamma\eta} \frac{N}{2\pi R_{\text{mach}}}. \quad (7.1)$$

It is not obvious how this should be generalized to bunched beams: should one replace $N/2\pi R_{\text{mach}}$ by the average density of protons per unit length of circumference, or by the peak density? They made the latter choice (which I believe is correct) and found qualitative agreement with their numerical results.

For further details, including figures displaying results of their super-particle calculations, the reader is referred to Lee and Teng's original paper.¹¹

7.3 Transverse Space-Charge Forces

The influence of transverse space-charge forces on the longitudinal dynamics is described by the terms $\varepsilon\lambda(\tau, \theta)p$ and $-\zeta Np$ in the single-particle equations of motion (4.43), (4.44). As discussed in Subsection 6.2, the term $-\zeta Np$ just shifts the transition by an amount which is the same for all particles, and its effect is therefore not very interesting. Moreover, this shift is very small, as it is made up entirely of image forces. We shall therefore not consider this term any further.

Let us first give a rough estimate¹⁴ of the effect of the term $\varepsilon\lambda(\tau, \theta)p$. Suppose the bunch is parabolic as given by Eq. (6.1). Then at the bunch centre

$$\lambda = \frac{3}{4} \frac{N}{h\theta}, \quad (7.2)$$

while at both ends of the bunch

$$\lambda = 0. \quad (7.3)$$

While the particles at the ends of the bunch would like the rf phase to be switched at $\tau = 0$ (neglecting now a $\gamma_{\text{transition}}$ -jump), the particles in the middle of the bunch, being less strongly focused, would prefer the phase to be switched at

$$\tau = -\varepsilon \frac{3N}{4h\hat{\theta}}. \quad (7.4)$$

In this way we have converted the transverse space-charge effect into an equivalent mistiming. Putting in numbers¹⁴ one finds $\tau = -0.03$ for the CERN PS with $N = 10^{12}$, and $\tau = -0.01$ (or less, depending upon the assumed transfer mode) for the CERN SPS with $N = 10^{13}$. From the linear theory, and from experiments as well, it is known that timing errors $|\Delta\tau|$ less than 0.25 or so are tolerable. The effect is therefore quite small.

In our estimate we have neglected the fact that particles move back and forth inside the bunch. It is not the same particle that always sits at the end of the bunch; now and then a particle which was once at the end will also visit the centre. Some smearing-out of the difference between end particles and central particles will probably take place, and the true effect is likely to be smaller than our estimate.

Germain¹⁵ has performed some super-particle calculations of this effect, including longitudinal space-charge forces, $\gamma_{\text{transition}}$ -jump and triple switch in the same calculation. As the purpose was not to study the negative-mass instability, he could neglect short-wavelength phenomena and was able to avoid bin-counting altogether. At every integration step he computed some chosen moments of the distribution and fitted an analytical distribution to reproduce the correct moments. In this way he could get sufficient accuracy with only a few hundred super-particles.

For the CERN PS with $N = 3 \times 10^{12}$ particles in the machine (the longitudinal space-charge parameter N_0 is then about 2.28 which means that the longitudinal space-charge forces are very important), he found that the transverse space-charge forces have indeed a negligible effect on the longitudinal dynamics.

8 EXPANSION-TYPE DESCRIPTION OF THE BUNCH MOTION

8.1 *The Expansion Method*

We shall now discuss another calculation of the negative-mass instability by a method which is

very different from the super-particle method used by Lee and Teng (Subsection 7.2). Both methods have their pros and cons. The expansion method is faster on the computer, and it is possible to provide the computer program with a device which makes it self-checking. It contains the ellipse description, Section 6, as a special case. On the other hand, much more mathematical work is necessary before one can start writing the computer program. The expansion method is therefore more inflexible if one wants to modify the equations of motion, to incorporate new effects, for instance. Moreover, it is not suitable if the distribution function develops steep gradients in phase space, as this leads to divergence problems.

The expansion method used is described in Ref. 58. The method is applied⁵⁹ to the Vlasov equation Eq. (5.2) with $\mu = \varepsilon = \zeta = 0$. For simplicity we linearize the rf force, but we keep the longitudinal space-charge term as it is. The Vlasov equation then becomes

$$\frac{\partial \rho}{\partial \tau} = -\tau p \frac{\partial \rho}{\partial \theta} - \left[\text{sgn}(\cos \phi_s)\theta + \xi \frac{\partial \lambda(\tau, \theta)}{\partial \theta} \right] \frac{\partial \rho}{\partial p}. \quad (8.1)$$

We suppose that ρ is approximately a two-dimensional Gaussian. The $1/e$ equidensity contour is then approximately an ellipse, with arbitrary shape and tilt. This approximate ellipse we transform into an approximate unit circle:

$$\begin{pmatrix} \tilde{\theta} \\ \tilde{p} \end{pmatrix} = \begin{pmatrix} \frac{1}{R\Theta} & 0 \\ -\frac{P}{R} & \frac{\Theta}{R} \end{pmatrix} \begin{pmatrix} \theta \\ p \end{pmatrix}. \quad (8.2)$$

The inverse transformation is

$$\begin{pmatrix} \theta \\ p \end{pmatrix} = \begin{pmatrix} R\Theta & 0 \\ RP & R/\Theta \end{pmatrix} \begin{pmatrix} \tilde{\theta} \\ \tilde{p} \end{pmatrix}. \quad (8.3)$$

Our assumption is that the $1/e$ contour of ρ is approximately elliptic in the (θ, p) system and approximately circular in the $(\tilde{\theta}, \tilde{p})$ system.

The matrix in Eq. (8.3) is the same one as the one used in the ellipse theory, Eq. (6.24), but this time we shall use equations of motion for R, Θ, P which are somewhat different from Eqs. (6.28).

We expand the distribution function ρ into a series of Hermite polynomials:

$$\begin{aligned}\rho(\tau, \theta, p) &= \frac{N}{hR^2} \frac{1}{\pi} \exp[-(\tilde{\theta}^2 + \tilde{p}^2)] \\ &\times \sum_{s=0}^m \sum_{i=0}^s a_{i,s-i}(\tau) H_i(\tilde{\theta}) H_{s-i}(\tilde{p}).\end{aligned}\quad (8.4)$$

We shall let R, Θ, P evolve with time in such a way that the pure Gaussian

$$\frac{N}{hR^2} \frac{1}{\pi} \exp[-(\tilde{\theta}^2 + \tilde{p}^2)] \quad (8.5)$$

has the same first and second-order moments as the true distribution, Eq. (8.4). To achieve this, the quantities R, Θ, P must obey the following equations of motion:

$$\left. \begin{aligned}\frac{d}{d\tau} R &= R c_{0,2} \\ \frac{d}{d\tau} \Theta &= \tau P - \Theta c_{0,2} \\ \frac{d}{d\tau} P &= \operatorname{sgn}(\cos \phi_s) \Theta \\ &+ \frac{\tau}{\Theta^3} + \frac{2}{\Theta} c_{1,1} - P c_{0,2}.\end{aligned}\right\} \quad (8.6)$$

$c_{i,j}$ denotes the following double sum over products of a 's:

$$\begin{aligned}c_{i,j} &= -\frac{\xi N}{hR^3 \Theta} \frac{1}{2^i i! \pi} \sum_{k=1}^{m+1} \sum_{l=0}^{m+1-j} \\ &\times a_{l,j-1} a_{k-1,0} GR_{i,k,l}.\end{aligned}\quad (8.7)$$

The factor $GR_{i,k,l}$ is defined by

$$\begin{aligned}GR_{i,k,l} &= \begin{cases} \pi^{-1} 2^{(1/2)(i+k+l-1)} \Gamma(\delta - i) \Gamma(\delta - k) \Gamma(\delta - l) \\ 0 \end{cases} \\ &\quad \begin{cases} \text{if } i + k + l = \text{even} \\ \text{if } i + k + l = \text{odd} \end{cases}\end{aligned}\quad (8.8)$$

with

$$2\delta = i + k + l + 1. \quad (8.9)$$

Even though the equations of motion (8.6) for R, Θ, P are quite simple, their derivation is rather lengthy and we shall not give it here. A detailed derivation is found in Ref. 59.

Suppose for a moment that we have a pure Gaussian, that is $a_{0,0} = 1$ and all other $a_{i,j} = 0$.

Equation (8.7) gives in this case

$$c_{0,2} = 0, \quad c_{1,1} = -\sqrt{\frac{1}{2\pi}} \frac{\xi N}{hR^3 \Theta}. \quad (8.10)$$

With a pure Gaussian therefore, Eqs. (8.6) degenerate into Eqs. (6.28) if we take the parameter N_0 to be

$$N_0 = \sqrt{\frac{2}{\pi}} \frac{\xi N}{hR^3}. \quad (8.11)$$

We should not be astonished that this expression for N_0 is not identical with Eq. (6.27), as the ellipse given by R, Θ, P is not the same one in the two cases.

We remark that while a distribution function giving linear space-charge forces will always keep this property, a pure Gaussian will not stay a pure Gaussian forever. Our requirement that the pure Gaussian (8.5) shall have the same first- and second-order moments as the true distribution (8.4) at all times, means that

$$\begin{aligned}a_{0,0} &= 1, \quad a_{1,0} = 0, \quad a_{0,1} = 0, \\ a_{2,0} &= 0, \quad a_{1,1} = 0, \quad a_{0,2} = 0\end{aligned}\quad (8.12)$$

at all times, that is, their time derivatives are zero. But the higher order a 's are not constant. With the notation

$$H_{i,j} = \frac{1}{\pi} \exp[-(\tilde{\theta}^2 + \tilde{p}^2)] H_i(\tilde{\theta}) H_j(\tilde{p}) \quad (8.13)$$

their equations of motion can be written as follows: for $s \geq 3$

$$\begin{aligned}&\sum_{i=0}^s \frac{d}{d\tau} a_{i,s-i} H_{i,s-i} \\ &= \sum_{i=0}^{s-1} \left\{ \left[-\left(\frac{\tau}{Q^2} + 2c_{11} \right) (i+1) a_{i+i,s-i-1} \right. \right. \\ &\quad \left. \left. - 2c_{02}(s-i) a_{i,s-i} + c_{i,s-i} \right] H_{i,s-i} \right\} \\ &\quad + \sum_{i=1}^s \left[\frac{\tau}{Q^2} (s-i+1) a_{i-1,s-i+1} H_{i,s-i} \right] \\ &\quad + \sum_{i=0}^{s-2} [-c_{02} a_{i,s-i-2} H_{i,s-i}] \\ &\quad + \sum_{i=1}^{s-1} [-c_{11} a_{i-1,s-i-1} H_{i,s-i}].\end{aligned}\quad (8.14)$$

The derivation of Eq. (8.14) is also given in Ref. 59.

If we solve the system of equations consisting of (8.6) and (8.14), we know how the distribution function $\rho(t, \theta, p)$ evolves with time.

8.2 Numerical Calculations on the Negative-Mass Instability¹²

A computer program¹² was written to integrate these equations of motion. As it is very difficult to imagine what the bunch looks like just by inspecting a table of coefficients, the program was also equipped with several forms of graphical output. It could, for instance, draw a contour plot of the distribution function, see Figure 14. On top of this contour plot is drawn (with a dashed line) the $1/e$ contour of that pure Gaussian which fits the true distribution to first- and second-order moments. In this way, one has an immediate feeling for the emittance of the bunch.

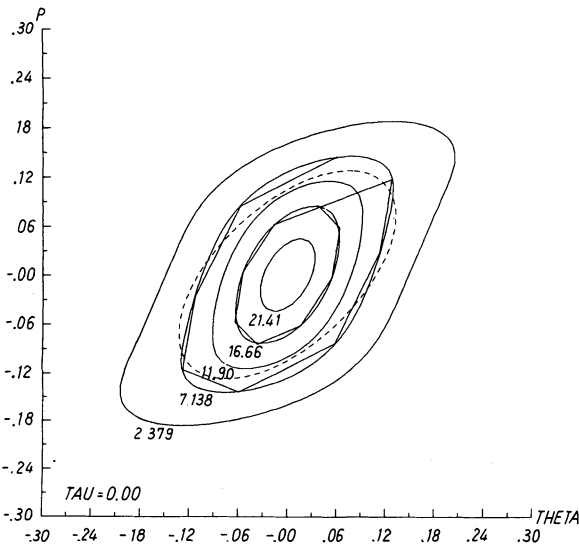


FIGURE 14 Contour plot of the distribution function (solid curves), with $1/e$ -contour of the best-fit Gaussian (dashed ellipse) and 16 test particles (piece-wise straight line). Parameters: CERN PS with $N = 10^{12}$ particles and cut-off limit $m = 20$.

If desired, the program can also follow the motion of a set of "test particles." The initial conditions of these test particles can be chosen by the user. Thereafter, they will move subject to the combined field of rf and space charge. The space-charge forces are worked out from the phase-space distribution $\rho(q, p)$ as described by the coefficients $a_{i,j}$; the test particles do not in any way interact with each other. The coordinates and

momenta of these test particles can be plotted on top of the contour plot. In order to know which test particle is which, so that one can see how they have moved from one snapshot to another, a straight line is drawn from number 1 to number 2, from 2 to 3, and so on to the last.

According to Liouville's theorem, the phase-space density at a given particle will always remain the same, if the equations of motion of the particles can be derived from a Hamiltonian (and this is the case with our problem). Therefore, if the initial conditions are chosen so that a test particle is sitting right on a certain density contour, it will always remain on this contour. The equations of motion for the single particles (for instance, of the test particles) and the equations of motion of the expansion coefficients look quite different, and the relation between them is rather indirect. (That is why Ref. 59 is such a long paper.) The test particles can therefore be used to check the accuracy of the computation: all sorts of inaccuracies (originating for instance from chopping off the infinite expansion) which make the test particles and the contour on which they were born depart from each other, are readily seen in the output.

Various runs with different combinations of particle number N and cut-off number m were performed.¹² The bunches were assumed to be symmetrical; this makes all coefficients $a_{i,j}$, with $i + j = \text{odd}$, equal to zero. The largest cut-off number which was tried was $m = 20$, which implies 121 coefficients with $i + j = \text{even}$. This means that we take into account about as many modes as Lee and Teng.

The runs started with a matched bunch with a pure Gaussian distribution at $\tau = -5$. Plotting was performed at $\tau = -5, -4, -3, \dots, 5$. The plotting routine (see Figure 14) attempted to plot the following contours: -10% of the central density, $+10\%$ of the central density, $+30\%$, $+50\%$, $+70\%$, $+90\%$, $+110\%$. The first and the last serve only test purposes: if such contours are seen, something must have gone wrong.

The computer calculations showed that a negative-mass instability develops after transition. In some cases the whole development of the instability could be followed right through the unstable time interval, in other cases only the beginning of it could be followed: if the distribution function develops steep gradients, thus deviating strongly from a Gaussian, the expansion will diverge. The test particles will warn us some time

before this happens by leaving the contour on which they were born.

As long as the expansion method is able to give meaningful results, a large number of terms give a better accuracy than a small number of terms. If, due to a well-developed instability, the gradients get so steep that the expansion breaks down, the catastrophe is more violent the larger the number of terms.¹² This is connected with the fact that the high-order modes grow fastest.

As we are not able to take into account sufficiently short wavelengths, the details of the numerical calculations¹² are not to be believed. The physical, qualitative results agree with those of the super-particle calculations,¹¹ Subsection 7.2.

9 SOME OTHER MECHANISMS AND ONE MORE CURE

9.1 Recapitulation

In Subsection 4.1 we listed various mechanisms which may influence the beam dynamics, along with various cures to combat their undesirable effects. In Sections 4 and 5 a coherent theory is developed for a subset of mechanisms and cures. In Sections 6 to 8 this theory is handled to various degrees of approximation. (Not all of these treatments deal with the full subset.)

In this section we shall discuss some mechanisms and cures which we have neglected until now for reasons of simplicity.

9.2 The Influence of Sextupolar Magnetic Fields

Already in 1956, Johnsen¹⁷ pointed out that if $\gamma_{\text{transition}}$ depends on the momentum of the individual particle, this will lead to a blow-up of the longitudinal emittance when transition is crossed. High-momentum particles and low-momentum particles cannot agree on when the phase should be switched. As we shall see, $\gamma_{\text{transition}}$ depends on the individual particle momentum even in a linear machine, but by adding some sextupole component to the main magnets or by the use of sextupoles, it is possible to get rid of this dependence.

A $\gamma_{\text{transition}}$ -jump will normally reduce the momentum spread of the bunch in the transition region. The same is true for a triple switch. Both these cures will therefore reduce the blow-up in question. We also remark that this blow-up is larger the greater the longitudinal emittance, while the opposite is

true for the blow-ups caused by longitudinal and transverse space-charge forces.

In the following we shall establish equations of motion taking into account the dependence of $\gamma_{\text{transition}}$ on the momentum of the individual particles. For simplicity we neglect all other blow-up mechanisms and all cures.

The equation of motion for the energy difference ΔE between the particle in question and the synchronous particle is not influenced by sextupolar fields and we can simply copy Eq. (4.1):

$$\frac{d}{dt} \left(\frac{\Delta E}{\omega_s} \right) = \frac{eV}{2\pi} (\sin \phi - \sin \phi_s). \quad (9.1)$$

The equation of motion for the phase ϕ is according to our definitions

$$\frac{d\phi}{dt} = -hc \left(\frac{\beta}{L} - \frac{\beta_s}{L_s} \right). \quad (9.2)$$

L is the orbit length for the particle in question and L_s is the orbit length for the reference particle. The minus sign in front of h is there because we measure ϕ backwards, see Subsection 4.2. Following Johnsen¹⁷ and Germain¹⁹ we assume that the orbit length for a particle with momentum $p_{\text{rel}} = p_s(1 + \xi)$ is given by†

$$L = L_s \{1 + \alpha_1 \xi + \alpha_1 \alpha_2 \xi^2 + O(\xi^3)\}. \quad (9.3)$$

If we neglect all terms of order ξ^2 , we find Eq. (4.2), but this time we shall keep all terms of order ξ^2 and only neglect terms of order ξ^3 . From relativistic mechanics alone we have by Taylor's formula

$$\beta = \beta_s \{1 + \gamma_s^{-2} \xi - \frac{3}{2}(\gamma_s^{-2} - \gamma_s^{-4})\xi^2 + O(\xi^3)\}. \quad (9.4)$$

Substitution gives

$$\begin{aligned} \frac{d\phi}{dt} = -h\omega_s &\{(\gamma_s^{-2} - \alpha_1)\xi + (\alpha_1^2 - \alpha_1 \alpha_2 - \alpha_1 \gamma_s^{-2} \\ &- \frac{3}{2}\gamma_s^{-2} + \frac{3}{2}\gamma_s^{-4})\xi^2 + O(\xi^3)\}. \end{aligned} \quad (9.5)$$

We assume that we are sufficiently close to transition so that we can put

$$\gamma_s = \gamma_{s,0} + \dot{\gamma}_{s,0} t. \quad (9.6)$$

γ_s is the γ of the synchronous particle at time t , $\gamma_{s,0}$ is the value of γ_s when the synchronous particle crosses transition. The instant when this happens

† p_{rel} denotes $mc\beta\gamma$.

is taken as the origin of time. This is substituted into Eq. (9.5), neglecting terms of order t^2 and of order $t\xi^2$. We then have

$$\begin{aligned} \frac{d\phi}{dt} = & -\hbar\omega_s \{ [\gamma_{s,0}^{-2} - \alpha_1 - 2\gamma_{s,0}^{-3}\dot{\gamma}_{s,0}t] \xi \\ & + [\alpha_1(\alpha_1 - \gamma_{s,0}^{-2}) - \alpha_1\alpha_2 - \frac{3}{2}\gamma_{s,0}^{-2} + \frac{3}{2}\gamma_{s,0}^{-4}] \xi^2 \\ & + 0(\xi^3)\}. \end{aligned} \quad (9.7)$$

From this formula we see that neglecting terms of order ξ^2 , $d\phi/dt$ is independent of ξ at $t = 0$ only if

$$\gamma_{s,0} = \alpha_1^{-1/2}, \quad (9.8)$$

which is the classical, first-order expression of, for instance, Courant and Snyder.³ With this relation substituted into Eq. (9.7), we have

$$\begin{aligned} \frac{d\phi}{dt} = & \hbar\omega_s \alpha_1 [2\gamma_{s,0}^{-1}\dot{\gamma}_{s,0}t + (\alpha_2 + \frac{3}{2} - \frac{3}{2}\alpha_1)\xi] \xi \\ & + 0(\xi^3). \end{aligned} \quad (9.9)$$

As before we introduce scaled variables τ and p to replace t and ξ . Substituting

$$t = T\tau \quad (9.10)$$

$$\xi = \beta_{s,0}^{-2}\gamma_{s,0}\Gamma p, \quad (9.11)$$

with the proportionality factors T and Γ given by Eqs. (4.41) and (4.42), the equations of motion take the simple form

$$\frac{d\theta}{d\tau} = (\tau + bp)p \quad (9.12)$$

$$\frac{dp}{d\tau} = \frac{\sin(\phi_s + \theta) - \sin\phi_s}{|\cos\phi_s|} \quad (9.13)$$

with

$$b = \frac{1}{2}(\alpha_2 + \frac{3}{2} - \frac{3}{2}\alpha_1)\beta_{s,0}^{-2}|\cotg\phi_s|. \quad (9.14)$$

As $\alpha_1 \ll 1$ it follows that $\beta_{s,0} \approx 1$ and we can write

$$b \approx \frac{1}{2}(\alpha_2 + \frac{3}{2})|\cotg\phi_s|. \quad (9.15)$$

Because the bunches are normally very short in the transition region we can as before linearize the equation of motion for p :

$$\frac{dp}{d\tau} = \text{sgn}(\cos\phi_s)\theta. \quad (9.16)$$

Let us imagine a particle with momentum $p_{\text{rel}} = p_s(1 + \xi)$, that is, with canonical momentum

p . When does this particle cross transition? It crosses transition when $d\theta/dt$ is insensitive to small variations of p around its actual value:

$$\frac{\partial}{\partial p} \left(\frac{d\theta}{d\tau} \right) = 0 \Rightarrow \tau = -2bp. \quad (9.17)$$

This result agrees with the one found by Johnsen.¹⁷

To estimate the size of the emittance blow-up by the nonlinear term, we regard a particle, the momentum of which deviates from the central one with a typical amount like $+ \sigma$ or $- \sigma$. One may also regard a particle at the "edge" of the bunch with a deviation $+2\sigma$ or -2σ . ($\pm 2\sigma$ is a good measure of bunch size, see Ref. 61.) We compute the corresponding mistiming as given by Eq. (9.17). This mistiming is substituted into the ellipse theory described in Section 6 and the oscillation amplitude found this way is taken as a measure of the longitudinal emittance blow-up. For the CERN PS, assuming $\phi_s = 58^\circ$, $\alpha_2 = 3.5$ and a bunch area $A = 0.07 \Delta\phi \times \Delta(\beta\gamma)$, we find $\tau = \pm 0.31$ for a typical particle and $\tau = \pm 0.62$ for an "edge" particle.¹⁹ This corresponds to emittance blow-up factors F of 1.29 and 1.70.

F is defined as follows: take the bunch length at a time τ_a after transition, when the length goes through a maximum. F is then given by

$$F = \frac{\text{length at time } \tau_a}{\text{length at time } -\tau_a}. \quad (9.18)$$

Experimentally,¹⁸ however, the CERN PS seems to be much more tolerant than this. The intensity of the machine was reduced to avoid all sorts of space-charge phenomena. The machine was then run with different sextupole currents. It is not known precisely which range of α_2 's was covered, but probably α_2 was varied in the range from about 1.5 to 5.5. No blow-up was observable within this range. Bunch lengths were measured to an accuracy of about $\pm 10\%$.

The estimate therefore does not agree too well with the experiment. In the estimate, the fact that $\gamma_{\text{transition}}$ for a given particle varies with time was not taken into account. But it seems likely that it is not just the value of $\gamma_{\text{transition}}$ at the instant of the phase jump which matters, but rather some sort of local average.¹⁴ This averaging process will reduce the blow-up. How much?

Germain¹⁹ has performed a super-particle calculation of the effect, handling the nonlinearity in a self-consistent way. As $\langle\theta\rangle = \langle p\rangle = 0$ is not a solution of the equations of motion (9.12), (9.16)

[†] p is the canonical conjugate to ϕ and is not $mc\beta\gamma$.

if $b \neq 0$, he introduced an extra term $-\langle \theta \rangle / \tau_c$ to simulate rf phase lock. The sign $\langle \rangle$ means averaging over all particles and τ_c is of the order of the normalized time-constant of the rf phase-lock loop. This is the only sort of coupling between particles in his model. All the difficulties of the superparticle method which we discussed in Section 7 are therefore avoided. For the CERN PS he found an $F = 1.08$, in agreement with experiment.

For the CERN SPS the situation is not quite so favourable. The value of α_2 is not known, so Germain gave his result as a function of α_2 . As ϕ_s is smaller, 45° instead of 58° , b is larger for the same α_2 . Even more important is the larger value of the longitudinal emittance, $A = 1.80 \Delta\phi \times \Delta(\beta\gamma)$ as compared to $0.007 \Delta\phi \times \Delta(\beta\gamma)$ in the PS. (The value $A = 0.180$ corresponds to bunch-by-bunch transfer; with continuous transfer it would be $A = 0.080$ or maybe even smaller.¹⁴⁾ The nonlinearity makes a sort of “bucket”, outside which particles are unstable. Already at $\alpha_2 = 0.5$ particles are lost due to the nonlinearity. The same value of α_2 gives an $F = 1.2$.

A calculation of the sextupole effect in the presence of a $\gamma_{\text{transition}}$ -jump, or a multiple phase switch, has not been carried out.

9.3 Coupling between Betatron Oscillations and Synchrotron Oscillations

Particles with large betatron amplitudes, radial or vertical, have a larger orbit circumference—at the same kinetic energy—than a particle with no betatron oscillations.²⁰ Even with beam control, the rf system cannot behave suitably for two kinds of particles simultaneously (probably the rf system will adjust itself to suit a particle with some kind of average betatron amplitude), and particles with large betatron amplitude will go through transition differently from particles with small betatron amplitude. This looks like a non-Liouvillean blow-up, an increase of longitudinal emittance, if one looks only at the longitudinal projection of the six-dimensional phase space.

The betatron oscillations will increase the circumference of the orbit from L to $L + \Delta L$; therefore $d\phi/d\tau$ will be different from zero even for a particle with $\Delta E = 0$. The equation of motion for ΔE , Eq. (4.1), is unchanged while the equation of motion for ϕ will have an extra term. The number of rf radians paced out per unit time by the rf wave is $h\omega_s$, and the number of rf radians paced out by a particle with $\Delta E = 0$ is $h\omega_s/(1 + \Delta L/L)$.

Dropping terms of second order in ΔL we have for a particle with $\Delta E = 0$:

$$\frac{d\phi}{dt} = h\omega_s \frac{\Delta L}{L}, \quad (\Delta E = 0). \quad (9.19)$$

For a particle with an energy different from the synchronous one we have

$$\frac{d\phi}{dt} = \frac{\eta h\omega_s \Delta E}{\beta^2 E} + h\omega_s \frac{\Delta L}{L}. \quad (9.20)$$

We linearize the rf force and introduce the same scaled variables τ and p as before. This gives

$$\frac{d\theta}{d\tau} = \tau p + \Lambda \quad (9.21)$$

$$\frac{dp}{d\tau} = \text{sgn}(\cos \phi_s) \theta \quad (9.22)$$

with

$$\Lambda = h \frac{\beta_{0,0} c}{R_{\text{mach}}} T \frac{\Delta L}{L}. \quad (9.23)$$

We note that Λ is a dimensionless quantity. Like $d\phi/d\tau$, it is measured in rf radians per unit interval of the scaled time τ .

The part of $d\theta/d\tau$ which comes from p (or ΔE) goes through zero and changes sign at transition, while the part Λ which is added due to betatron oscillations is always positive. An asymmetry will therefore occur.

Let us take a look at numerical values. An analysis of the betatron oscillations in the CERN PS gave $0 \leq \Delta L/L \leq 1.0 \times 10^{-7}$, which is a very small number. During the time in which the rf system turns one radian, a perturbation of θ is produced; this perturbation is equal to $\Delta L/L$ rf radians. But transition lasts for a time T which is long compared to the time in which the rf system turns one radian, in fact 1.2×10^5 times longer. This gives a $0 \leq \Lambda \leq 1.2 \times 10^{-2}$, which is not so small.

If the solution well before transition is, with the notation of Eq. (6.30),

$$\theta = |\tau|(A_J J + A_N N), \quad (-\tau \gg 1), \quad (9.24)$$

it can be shown analytically²⁰ that well after transition

$$\theta = |\tau|(A'_J J + A'_N N), \quad (\tau \gg 1), \quad (9.25)$$

with the new amplitudes related to the old ones by the equations

$$\left. \begin{aligned} A'_J &= A_J + \frac{2\pi}{3\sqrt{3}} \Lambda \\ A'_N &= A_N - \frac{2\pi}{3} \Lambda. \end{aligned} \right\} \quad (9.26)$$

J and N are given by Eqs. (6.30). We assume that the rf system adjusts itself to a particle with an average amount of betatron oscillations, and that synchrotron oscillations and betatron oscillations are uncorrelated, so that for every A_J , A_N there is a spectrum of Λ 's between 0 and 1.2×10^{-2} . With parameters of the CERN PS this gives an emittance blow-up of about 5%.

Gareyte⁶² has performed an experiment on the CERN PS. He reduced the beam intensity to avoid all space-charge phenomena. This beam has less betatron oscillations than the full-intensity beam if no special tricks are carried out, but by double-pulsing the inflector the amount of betatron oscillations was artificially increased to about its normal value. No blow-up was observed. The reason for the disagreement is not known. A possible explanation is that the betatron amplitudes are smaller than the numbers used in the calculation; they are not so easy to measure with precision.

9.4 Coupling to the Rf Cavities ("Beam Loading")

This effect has been studied theoretically by Balbekov and Pashkov.¹⁶

When the beam current passes through an rf cavity, a voltage is induced across the acceleration gap. The corresponding force is a longitudinal space-charge force of a similar nature to the one studied in Subsection 4.3. Its main influence on the beam dynamics is to set up bunch-length oscillations similar to those studied in Section 6. However, the single-particle equations are nonlinear, and some bunch distortion will also occur. Due to the nonlinearity the ellipse formalism is not suitable.

An rf cavity is a rather complicated device. In addition to its main resonance, it usually also has higher resonances. The position and strength of these higher resonances depend on how the cavity is constructed. For calculations like the present one it is desirable to use a simplified model of the cavity impedance as a function of frequency. Balbekov and Pashkov replaced the cavity by its

gap impedance, neglecting all higher resonances. They were interested in the Serpukhov 70-GeV accelerator; their approximation may or may not be a good one for a given machine.

The voltage induced in the cavity by the beam contains only harmonics of the rf (as long as the bunch shape varies slowly compared to a period of the rf, as is the case). The dc component is zero. Most accelerators have a feedback system to keep the first harmonic at a given level. Therefore we only have to take into account the second and higher harmonics. The fact that $Z = 1/(i\omega C)$ is a very bad approximation for the first harmonic does not matter, as long as it is sufficiently good for the second, third and so on.

As before we let $\lambda(\theta)$ denote the number of particles per rf radian in the vicinity of θ . The beam current through the cavity is then $(e\beta ch/R_{\text{mach}})\lambda(\theta)$. This current will produce a voltage across the gap

$$\tilde{V}(t) = -\frac{1}{C} (e\beta ch/R_{\text{mach}}) \int \tilde{\lambda}(\theta) dt. \quad (9.27)$$

The tilde means that the zeroth and the first harmonic of the corresponding quantity are to be neglected. Suppose there are M cavities along the circumference. The extra energy gain per turn is then $eM\tilde{V}(t)$. Substituting $t = (R_{\text{mach}}/\beta ch) \theta$ the total energy gain per turn is, using what we found in Section 4:

$$\begin{aligned} eV \sin \phi + & \frac{2\pi h^2 g_0}{\gamma_{0,0}^2} \frac{r_p}{R_{\text{mach}}} mc^2 \frac{d\lambda(\theta)}{d\theta} \\ & - \frac{e^2 M}{C} \int \tilde{\lambda}(\theta) d\theta. \end{aligned} \quad (9.28)$$

The first term is due to the imposed rf field, the second term is due to the capacity between the beam and the vacuum chamber, the third term is due to the coupling with the cavities. We notice that while $d\lambda/d\theta$ contains more high-frequency components than λ , $\int \lambda d\theta$ contains less high-frequency components than λ . When studying beam loading it is therefore not necessary to take into account very short wavelengths, despite the fact that even a parabolic bunch produces nonlinear forces, as we shall see in a moment.

We take a bunch like Eq. (6.1), assuming that the bunch is short compared to the distance between two bunches. This is substituted into the expression (9.28) for the energy gain per turn, which will replace $eV \sin \phi$ in the equation of motion, Eq. (4.1). Scaled variables τ and p are

introduced as before, Eqs. (4.39) and (4.40). The equations of motion then are

$$\frac{d\theta}{d\tau} = \tau p \quad (9.29)$$

$$\begin{aligned} \frac{dp}{d\tau} &= \text{sgn}(\cos \phi_s \theta - \frac{3 N \xi}{2 h \hat{\theta}^3} \theta) \\ &- \frac{3}{4 h e V |\cos \phi_s| C} \left[\frac{\theta}{\hat{\theta}} - \frac{1}{3} \left(\frac{\theta}{\hat{\theta}} \right)^3 \right]. \end{aligned} \quad (9.30)$$

Balbekov and Pashkov solved these equations on a digital computer by means of a sort of super-particle technique. They used 32 super-particles all situated on the boundary of the bunch. Each super-particle moved according to Eqs. (9.29), (9.30). At every integration step the particles were investigated to find the one with the largest θ , and $\hat{\theta}$ was put equal to this currently largest θ . The technique is similar to the fitting method of Germain,¹⁵ described in Section 7.3.

They present solutions for many different combinations of parameters. For the Serpukhov machine the amount of bunch distortion with beam loading only (longitudinal space-charge forces switched off) is about half as large as with longitudinal space-charge forces alone. The distortion with both mechanisms present is roughly equal to the sum of their individual contributions; Eq. (9.30) also indicates that they add constructively. The coupling with the rf cavities is therefore an effect which should not be neglected.

Balbekov and Pashkov state that taking into account not only the capacitance of the cavity, but also its inductance and resistance, would give a 20 to 25% larger effect. They do not discuss higher resonances. For graphical and numerical results the reader is referred to their original paper.¹⁶

From Eq. (9.30) it is seen that increasing the bunch length will reduce the cavity force compared to the rf force. However, the reduction factor for the main term is only $\sim 1/\hat{\theta}$, while for longitudinal space-charge force the reduction factor is $\sim 1/\hat{\theta}^3$. This means that $\gamma_{\text{transition}}$ -jump will help to cure the cavity effect, but not as efficiently as it cures the longitudinal space-charge effect.

9.5 Continuous rf Matching

Let V_N and ϕ_N denote the nominal values of V and ϕ_s after transition. Up to transition the normal

rf programme is used, $V = V_N$, $\phi_s = \pi - \phi_N$. To retain a solution which is symmetric around transition, we adjust V and ϕ_s after transition in such a way that the total focusing force (rf + space charge) is the same after transition as it was at the corresponding point before transition, while the rate of acceleration is kept constant all the time:

$$V \sin \phi_s = V_N \sin \phi_N \quad (9.31)$$

$$V \cos \phi_s = f V_N \cos \phi_N. \quad (9.32)$$

f denotes the factor by which the rf focusing force is reduced compared to its nominal value after transition. We shall now establish which programme f must follow in order to give a symmetrical solution. With a general $f(t)$ we find by the methods of Section 6:

$$\left. \begin{aligned} \frac{d\Theta}{d\tau} &= \tau P \\ \frac{dP}{d\tau} &= -f\Theta - \frac{N_0}{\Theta^2} + \frac{\tau}{\Theta^3}. \end{aligned} \right\} \quad (9.33)$$

These equations contain the triple switch or multiple switch as a special case: f is then alternatively -1 and $+1$, compare Eqs. (6.28). We now demand that $\Theta(\tau)$ be symmetrical:

$$\Theta(\tau) = \Theta(-\tau). \quad (9.34)$$

This implies

$$\begin{aligned} f(\tau) &= -f(-\tau) - \frac{2N_0}{[\Theta(-\tau)]^3} \\ &= 1 - \frac{2N_0}{[\Theta(-\tau)]^3}, \quad t > 0. \end{aligned} \quad (9.35)$$

With exactly this rf programme, the solution will be exactly symmetrical. However, a numerical sensitivity analysis²⁶ showed that with this way of crossing transition the solution is very sensitive to small errors in the rf programme. An rf programme was constructed corresponding to $N_0 = 2.3$. The equation of motion was then solved with this $f(\tau)$ but with an N_0 which was 10% larger or smaller than the rf programme "expected." This relatively small amount of intensity fluctuations resulted in bunch distortions F up to 2.4, with F as defined by Eq. (9.18). This method does not seem to have any advantages over the triple switch method.

It shares with the triple switch method the

difficulty that while $f < 0$ the bunches are position-unstable and will rush off in all directions.

10 THE STATE OF TODAY'S KNOWLEDGE

During the last few years we have got much more detailed insight into what happens when the phase transition is crossed. We feel we completely understand the mechanisms causing the bunch-length oscillations, and we have at least a qualitative understanding of the mechanisms causing blow-up of the longitudinal emittance. There is even a long list of cures for these undesirable effects, and some of these cures have been experimentally shown to work, at least under the circumstances under which they were tried. But there are still many things we should like to know better.

We do not have a dynamical[†] calculation that permits us to follow in detail the development of the negative-mass instability right through the unstable range. Present-day calculations only include the longer wavelengths, even though theoretical arguments³⁰ indicate that the fastest growth takes place with very short wavelengths, only about 1 cm long, see Subsection 7.2. However, the stability limit (at least for infinitesimal amplitude) is independent of wavelength³⁰: either all modes are stable, or all modes are unstable. Therefore a calculation only including the longer wavelengths at least gives us some insight into the problem.

All dynamical calculations of instability phenomena are difficult to perform with precision: by their very nature, all computational noise will grow exponentially (or in a similar way). The negative-mass problem is particularly difficult, with very many modes that couple to each other by nonlinearities. A small-amplitude theory will not do to compute the amount of blow-up in a given case. Hereward⁶³ has suggested using fluid-dynamics techniques, where one puts the infinite discontinuities into the lowest order of approximation. So far, nobody has been able to carry this out. With a detailed dynamical calculation one could predict the limitations of a future machine, or one could predict the limitations of a proposed cure for an already existing machine.

[†] A calculation is called dynamical if it follows the motion of the system with time. The opposite, a *static* calculation, only makes statements about the initial state, for instance whether it is stable or not, or initial growth rates.

Passive compensation by modification of the electromagnetic environment of the beam appears to be a very interesting method. More detailed work is necessary here, both theoretical and experimental, especially on the high-frequency behaviour of such devices. One has to compensate correctly for wavelengths from about one bunch length down to about one chamber diameter divided by γ . For the CERN PS, this means from about 3 m down to 1 cm. This is certainly no easy problem. Especially, one must be careful not to over-compensate; this seems to be worse than under-compensation, see Subsection 3.5 and Ref. 8.

Let us now turn to the experimental side. Rather few experiments have been performed, virtually all of them on the CERN PS. This is apparently the only machine which has sufficiently broad-banded beam observation equipment to do precision work of this type. (Moreover, the incentive to reduce blow-up at transition has been larger with this machine, as it is used as injector for a set of storage rings.) This is unfortunate, as in other machines with other parameters, unobserved and unknown phenomena may take place. The highest frequencies which can be observed in the CERN PS are about 600 MHz (or maybe a little higher), which corresponds to 0.5 m. This means that experimentally one is no better off than one is theoretically as far as the study of short-wavelength phenomena is concerned.

In all experimental work available today, one has only observed the projected distribution $\lambda(\theta)$ but not the phase-space distribution $\rho(\theta, p)$. One could imagine performing a fast ejection of the circulating beam. The ejected beam is guided through a magnet for momentum analysis, a magnet with vertical bending, say. At the same time the beam is swept horizontally by another magnet, which has in fact to be another fast kicker. Finally, the beam is detected by a fluorescent screen (or by a photographic film). On this screen the θ -coordinate is displayed horizontally and the p vertically. Different ρ 's are seen as different degrees of brightness. However, such an experiment is no easy set-up. (One could avoid the external kicker by just time-analysing on an oscilloscope a narrow momentum slice. The complete picture would then have to be built up by many successive machine pulses, which is less satisfactory.) Observations of the phase-space distribution may yield much more detailed information on the mechanisms at work.

ACKNOWLEDGEMENTS

Many of the important ideas about transition phenomena have come to the surface in discussions between interested people, and it is sometimes difficult to say who contributed what. For instance, no single person seems to have invented the $\gamma_{\text{transition}}$ -jump, the most successful of all cures. However, it is clear that such ideas do not come out of the air by themselves. Sincere thanks to all contributors, even though I cannot always name them. I am especially grateful to H. G. Hereward who introduced me to the topic and ever since has been a constant source of inspiration. I am also very grateful to my colleagues in the Machine Studies Team at the CERN-MPS Division.

REFERENCES

1. K. Johnsen, The Phase Equation in the Transition Region, CERN-PS/KJ 22 (CERN, Bergen, 1953).
2. L. L. Goldin and D. G. Koshkarev, *Nuovo Cimento*, **2**, 1251 (1955).
3. E. D. Courant and H. S. Snyder, *Ann. Phys. (USA)*, **3**, 1 (1958).
4. J. Gareyte, private communication.
5. J. C. Maxwell, *Adams Price Essay (1856)*, *Scientific Papers* (Cambridge University Press, Cambridge, 1890; reprinted by Dover Publications Inc., New York, 1965), p. 288.
6. V. V. Vladimirska and E. K. Tarasov, *Theoretical Problems of the Ring Accelerators* (USSR Academy of Sciences, Moscow, 1955).
7. L. C. Teng, *Particle Accelerators*, **4**, 81 (1972).
8. A. Sørensen, The effect of Strong Longitudinal Space-Charge Forces at Transition, MPS/Int. MU/EP 67-2 (CERN, Geneva, 1967).
9. W. Hardt and A. Sørensen, How to Pass Transition in the CPS at High Intensity? Part 2: Beam Dynamics, CERN/MPS/DL, 71-6 (CERN, Geneva, 1971).
10. W. Hardt, G. Merle, D. Möhl, A. Sørensen, and L. Thordahl, *Proc. 7th Int. Conf. on High-Energy Accelerators, Yerevan, 1969* (The Publishing House of the Academy of Sciences of Armenian SSR. Yerevan, 1970), Vol. 2, p. 329.
11. W. W. Lee and L. C. Teng, *Proc. 8th Int. Conf. on High-Energy Accelerators, Geneva, 1971* (CERN, Geneva, 1971), p. 327.
12. A. Sørensen, What Happens Right After Phase Transition, CERN/MPS/DL 72-14 (CERN, Geneva, 1972).
13. H. H. Umstätter, private communication.
14. A. Sørensen, *Spring Study on Accelerator Theory*, AMC-1 (CERN, Geneva, 1972), p. 49.
15. P. Germain, A simulation method to estimate the effect of the transverse space-charge forces at transition, CERN/MPS/DL 73-8 (CERN, Geneva, 1973).
16. V. I. Balbekov and P. T. Pashkov, Interaction of an intense beam with the cavities of the acceleration stations at transition, IFVE SKU 71-72 (IHEP, Serpukhov, 1971), in Russian. [English translation: CERN Trans. 72-15 (CERN, Geneva, 1972).]
17. K. Johnsen, *Proc. CERN Symposium on High-Energy Accelerators and Pion Physics, Geneva, 1956* (CERN, Geneva, 1956). Vol. 1, p. 106.
18. B. Frammery, J. Gareyte, P. Germain and A. Sørensen, Mesures de l'effet de la chromacité sur le passage de la transition, MPS/CO/MD 72-5 (CERN, Geneva, 1972).
19. P. Germain, Effect of magnetic field non-linearities at transition on bunch length, CERN/MPS/DL 72-13 (CERN, Geneva, 1972).
20. H. G. Hereward and A. Sørensen, Longitudinal blow-up of the bunches at transition, caused by coupling between synchrotron oscillations and betatron oscillations, MPS/Int. DL, 68-3 (CERN, Geneva, 1968).
21. A. Sørensen and H. G. Hereward, Longitudinal space-charge forces at transition, MPS/Int. MU/EP 66-1 (CERN, Geneva, 1966).
22. W. Schnell, private communication.
23. A. Sørensen, "The triple switch"—a method of compensating longitudinal space-charge forces at transition, MPS/Int. MU/EP 66-2 (CERN, Geneva, 1966).
24. J. Jamsek, private communication.
25. J. Gareyte, private communication.
26. A. M. Sessler and A. Sørensen, unpublished.
27. R. J. Briggs and V. K. Neil, Plasma phys.—Accelerators—Thermonuclear research (*J. Nuclear Energy*, Part C), **8**, 255 (1966).
28. The CERN study group on new accelerators, Report on the design study of a 300 GeV proton synchrotron, AR/Int. SG/64-15 (CERN, Geneva, 1964), vol. 1, p. 62.
29. A. M. Sessler and V. G. Vaccaro, Passive compensation of longitudinal space-charge effects in circular accelerators: The helical insert, CERN 68-1 (CERN, Geneva, 1968).
30. V. K. Neil and A. M. Sessler, *Rev. Sci. Instrum.*, **36**, 429 (1965).
31. E. D. Courant, Longitudinal space-charge effects at transition in NAL booster and main ring, FN-187/0300 (NAL, Batavia, 1969).
32. E. C. Raka, *IEEE Trans. Nuclear Sci.*, **NS-16**, No. 3, 182 (1969).
33. D. Boussard, Une présentation élémentaire du système "beam control" du PS, MPS/SR/note/73-10 (CERN, Geneva, 1973).
34. A. Sørensen, *Proc. 6th Int. Conf. on High-Energy Accelerators, Cambridge, Mass. 1967* (CEA, Cambridge, Mass., 1967), p. 474.
35. L. C. Teng, Compensation of space-charge mismatch at transition of booster using the transition-jump method, FN-207/400 (NAL, Batavia, 1970).
36. D. Möhl, Compensation of space-charge effects at transition by an asymmetric Q-jump: A theoretical study, CERN-ISR/300/GS/69-62 (CERN, Geneva, 1969).
37. W. Lee and L. C. Teng, Numerical study of beam bunch length matching at transition using the γ_t -jump method, FN-215/0100 (NAL, Batavia, 1970).
38. W. Lee and L. C. Teng, Addendum, FN-215-A/0100 (NAL, Batavia, 1970).
39. L. C. Teng, Arrangements of pulse quadrupoles in the main ring for γ_t -jump, TM-276/0402 (NAL, Batavia, 1970).
40. W. W. Lee and L. C. Teng, *IEEE Trans. Nuclear Sci.*, **NS-18**, No. 3, 1057 (1971).
41. H. G. Hereward, Estimates of bunch lengths and longitudinal space-charge forces in the CPS, MPS/DL Int. 66-3 (CERN, Geneva, 1966).
42. P. L. Morton, *Rev. Sci. Instrum.*, **36**, 1826 (1965).
43. C. E. Nielsen, A. M. Sessler and K. R. Symon, *Proc. Int. Conf. on High-Energy Accelerators, Geneva, 1959* (CERN, Geneva, 1959), p. 239.
44. A. Sørensen, Vlasov equation at transition with transverse and longitudinal space-charge forces, CERN/MPS/DL 72-3 (CERN, Geneva, 1972).
45. L. J. Laslett, *Proc. 1963 Summer Study on Storage Rings*,

- Accelerators and Experimentation at Super-High Energies, Brookhaven, 1963*, BNL 7534 (Brookhaven, 1963), p. 324.
46. H. G. Hereward and K. Johnsen, On the phase equations for synchrotrons, CERN-PS/HGH-KJ1 (CERN, Geneva, 1957).
 47. L. Thorndahl, Q-jump pulser for transition experiments, ISR-300/LI/69-38 (CERN, Geneva, 1969).
 48. W. Hardt, How to pass transition in the CPS at high intensity? Part 1: A large change of γ_{tr} , CERN/MPS/DL 70-16 (CERN, Geneva, 1970).
 49. W. Hardt and H. Schönauer, How to pass transition in the CPS at high intensity? Part 3: A large change of γ_{tr} without Q-change, CERN/MPS/DL 71-1 (CERN, Geneva, 1971).
 50. W. Hardt, H. Schönauer and A. Sørenssen, *Proc. 8th Int. Conf. on High-Energy Accelerators, Geneva, 1971* (CERN, Geneva, 1971), p. 323.
 51. H. Schönauer, Lens configurations for the CPS to provide a large and fast γ_{tr} -jump without Q-change, CERN/MPS/DL 72-7 (CERN, Geneva, 1972).
 52. H. H. Umstätter, The minimum length and shape of proton bunches at transition at high and low beam intensity, MPS/SR-Note 69-11 (CERN, Geneva, 1969).
 53. M. Bell, Creating bunches of random points in a phase plane with a given projected distribution, CERN/MPS/DL 73-3 (CERN, Geneva, 1973).
 54. F. Sacherer, private communication.
 55. I. M. Kapchinskij and V. V. Vladimirkij, *Proc. Int. Conf. on High-Energy Accelerators, Geneva, 1959* (CERN, Geneva, 1959), p. 274.
 56. W. E. K. Hardt and A. Sørenssen, Reduction of synchrotron beam width at transition by multiswitch, MPS/DL Note 71-4 (CERN, Geneva, 1971).
 57. B. Alder, S. Fernbach and M. Rotenberg (Eds.), *Methods in Computational Physics*, Vol. 9, Plasma Physics (Academic Press, New York, 1970).
 58. A. Sørenssen, *Proc. 8th Int. Conf. on High-Energy Accelerators, Geneva, 1971* (CERN, Geneva, 1971), p. 348.
 59. A. Sørenssen, Continuous adjustment of the zeroth approximation in an expansion method for calculating space-charge dynamics, CERN/MPS/DL 72-6 (CERN, Geneva, 1972).
 60. A. N. Lebedev, *Proc. 6th Int. Conf. on High-Energy Accelerators, Cambridge, Mass., 1967* (CEA, Cambridge, Mass., 1967), p. 284.
 61. P. M. Lapostolle, Quelques propriétés essentielles des effets de la charge d'espace dans des faisceaux continus, CERN-ISR/DI-70-36 (CERN, Geneva, 1970).
 62. J. Gareyte, Comptes rendus de machine development, Mesures à transition, MPS/CO (CERN, Geneva, 1968).
 63. H. G. Hereward, *Proc. 8th Int. Conf. on High-Energy Accelerators, Geneva, 1971* (CERN, Geneva, 1971), p. 548.